

Developmental Osteology of the Parafrontal Bones of the Sphaerodactylidae

AARON H. GRIFFING  ^{1,*} JUAN D. DAZA,² JONATHAN C. DEBOER,¹
AND AARON M. BAUER¹

¹Department of Biology, Villanova University, 800 Lancaster Avenue, Villanova, Pennsylvania

²Department of Biological Sciences, Sam Houston State University, 1900 Avenue I, Huntsville, Texas

ABSTRACT

Well-resolved phylogenetic hypotheses and ontogenetic data are often necessary for investigating the evolution of structural novelty. The Sphaerodactylidae comprises 12 genera of predominantly miniaturized geckos. The genera *Aristelliger* and *Teratoscincus* are exceptions, with taxa reaching snout-to-vent lengths far exceeding those of other sphaerodactylids. These two genera possess enigmatic, supraorbital ossifications—parafrontal bones—which are encountered nowhere else among squamates. At the time of their discovery, these structures were believed to be the result of evolutionary convergence. Although relationships between other sphaerodactylids remain unresolved, recent molecular and morphological data have supported a close relationship between *Aristelliger* and *Teratoscincus*. We investigated the ontogeny of parafrontal bones to better understand relationships between sphaerodactylid body size and the presence of parafrontals, and to evaluate whether ontogenetic data support the homology of parafrontals between *Aristelliger* and *Teratoscincus*. We hypothesize that the parafrontals of *Aristelliger* and *Teratoscincus* are homologous and that there is a threshold body size in sphaerodactylids below which parafrontals do not develop, thus explaining their absence from the miniaturized taxa. The presence of parafrontals was investigated in all sphaerodactylid genera using cleared-and-stained, radiographed, and skeletonized specimens. Total surface area of parafrontals was measured for seven species of *Aristelliger* and six species of *Teratoscincus* throughout their ontogeny. Histology was used to investigate the cellular composition of the parafrontals throughout their ontogeny. Our data suggest that parafrontals have evolved in parallel from a homologous, parafrontal precursor and that the onset of parafrontal development is not strictly dependent on a threshold body size. Anat Rec, 301:581–606, 2018. © 2017 Wiley Periodicals, Inc.

Key words: gecko; supraorbital; circumorbital bones; ossa parafrontalia; homology

Additional Supporting Information may be found in the online version of this article.

*Correspondence to: Aaron H. Griffing, Department of Biological Sciences, Marquette University, 530 15th Street, Milwaukee, WI 53233. E-mail: aaron.griffing@marquette.edu

Received 14 June 2017; Revised 23 October 2017; Accepted 31 October 2017.

DOI 10.1002/ar.23749

Published online 12 December 2017 in Wiley Online Library (wileyonlinelibrary.com).

Novel structures facilitate evolutionary diversification in organisms; however, the origins of these unique traits are often poorly understood (Goldschmidt, 1940; Gould, 2002; Moczek, 2005, 2008; Moczek et al., 2006). Of fundamental interest is the identification and understanding of the evolution of homoplastic versus homologous characters, which requires the utilization of phylogenetic data to corroborate or falsify common ancestry, and developmental data to determine the mechanism of differentiation (Wake et al., 2011). Recently, increased resolution of phylogenetic hypotheses within gekkotans (geckos) has revealed well-supported, sometimes novel, relationships (Gamble et al., 2008a; 2008b; 2012; 2015a; 2015b). These results support the repeated, independent evolution of several important complex traits, including temporal activity, sex determining mechanisms, and adhesive toepads (Gamble et al., 2012, 2015a, 2015b), and have implications for additional questions about homology and homoplasy.

The Sphaerodactylidae is a gekkutan family within which a variety of life histories and ecological traits are expressed. It is distributed across South America, the Caribbean, northern Africa, and the Middle East (Gamble et al., 2008a). Sphaerodactylids comprise roughly 13% of described extant geckos (Uetz et al., 2017), and most species are characterized by their derived miniaturized condition (Rieppel, 1984a). Examples include *Sphaerodactylus parthenopion* (18 mm maximum snout-to-vent length [SVL]; Schwartz and Henderson, 1991), *S. elasmorhynchus* (17 mm maximum SVL), and *S. ariasae*, which, until recently (Glaw et al., 2012), was the smallest described amniote, averaging 16 mm SVL (Hedges and Thomas, 2001). The Sphaerodactylinae (*sensu* Gamble et al., 2008a) comprises the Old World miniaturized genus *Sauromactylus* and its sister clade, the New World miniaturized Sphaerodactylini (*Chatogekko*, *Coleodactylus*, *Gonatodes*, *Lepidoblepharis*, *Pseudogonatodes*, and *Sphaerodactylus*; Gamble et al., 2008a; Guerra-Fuentes et al., 2014). Members of this group have lightly-built skulls (Daza et al., 2008; Gamble et al., 2011b) and generally exhibit extremely small adult body sizes. Of the 171 described sphaerodactyline species, only *Lepidoblepharis grandis* and nine species of *Gonatodes* reach sizes exceeding 50 mm SVL (Fig. 1). Furthermore, this clade can be characterized as miniaturized based on cranial morphology (skull length \leq 15 mm, the braincase being co-planar with the parietals, and closure of the post-temporal fossae; Rieppel, 1984a; Daza et al., 2008). *Pristurus*, the Old World sister lineage to the Sphaerodactylinae, comprises 25 species, only five of which reach sizes exceeding 50 mm SVL (e.g., *Pristurus carteri*; Fig. 1). The remaining members of the family (*Aristelliger*, *Euleptes*, *Sauromactylus fasciatus*, *Teratoscincus*, and *Quedenfeldtia*) are primarily distributed in the Old World (with exception to *Aristelliger*) and exhibit a variety of body sizes. Though *Euleptes*, *S. fasciatus*, and *Quedenfeldtia* also exhibit extremely small adult sizes (38–45 mm maximum SVLs), they are not miniaturized as they do not exhibit leveling of the braincase with the parietals or closure of the post-temporal fossae. Obvious exceptions to miniaturization occur in the genera *Teratoscincus* and *Aristelliger* (Fig. 1). The maximum SVLs of *Teratoscincus* range between 73 and 116 mm (*T. microlepis* and *T. keyserlingii*, respectively; Anderson, 1999; Szczerbak and Golubev, 1996), whereas the SVL range

of *Aristelliger* is 50–135 mm (Schwartz and Henderson, 1991). This range is the largest among sphaerodactylids and overlaps with other sphaerodactylid genera (Fig. 1).

Underwood (1954) originally placed *Coleodactylus*, *Gonatodes*, *Lepidoblepharis*, *Pseudogonatodes*, and *Sphaerodactylus* in the Sphaerodactylidae, although he noted that these miniaturized geckos shared traits such as rounded pupils with what are now considered Old World sphaerodactylids. Subsequent systematic work on geckos supported the monophyly of the miniaturized sphaerodactylids *sensu* Underwood (1954) (Kluge, 1967, 1987, 1995; Han et al., 2004). The expansion of the Sphaerodactylidae beyond Underwood's hypothesis occurred when Gamble et al. (2008a) re-elevated *Sphaerodactylus* and its New World allies to the familial level, the Sphaerodactylidae. This revision also added the New World genus *Aristelliger* and the Old World genera *Sauromactylus*, *Quedenfeldtia*, *Pristurus*, *Euleptes*, and *Teratoscincus* to the family, stabilizing the current composition. These newly included taxa lie basal to the Sphaerodactylini or occupy a different familial branch. Subsequent analyses by Gamble et al. (2008b; 2012; 2015b) and Pyron et al. (2013) place sphaerodactylids as sister to the clade of Gekkonidae + Phyllodactylidae. Although the higher-level placement of the Sphaerodactylidae is well resolved, there is disagreement with regard to generic-level hypotheses, with recent molecular phylogenies recovering varying positions for *Euleptes*, *Pristurus*, and *Sauromactylus* (Gamble et al., 2011a, 2011b, 2015b).

The gekkutan *Bauplan* has been considered to be plesiomorphic among squamates (Conrad, 2004). Gekkutan cranial morphology, however, is derived and specialized relative to that of other extant squamates (Kluge, 1983; Rieppel, 1984b; Herrel et al., 2000; Daza and Bauer, 2010; Gamble et al., 2012). In the Sphaerodactylidae, *Aristelliger* and *Teratoscincus* possess enigmatic, novel supraorbital ossifications: parafrontal bones, or *ossa parafrontalia* (Bauer and Russell, 1989). As originally described, these elements take the form of roughly 15–30 bony plates lacking cartilaginous components in the supraorbital region of the skull, held together by connective tissue. In *Teratoscincus* the bony plates are thin (mean = 108 μm , N = 30 sections; Bauer and Russell, 1989), rugose, highly irregular in shape, extend from the rim of the orbit into the extra-brillar fringe (*sensu* Bellairs, 1948), and lie in the same plane as the frontal and prefrontal bones (Fig. 2). Bauer and Russell (1989) originally described the connective tissue covering the dorsal surface of the bony plates, as well as the interstices between them, as mesenchyme. We acknowledge that this highly vacuolar tissue is not an embryonic mesh-work, but rather a supraorbital, fibrous connective tissue sheet of probable mesenchymal origin. Parafrontal bones of *Aristelliger* are similar in position to those of *Teratoscincus*, but do not extend as far into the extra-brillar fringe, are smoother, less irregular in shape, and are separated by smaller interstices. These interstices are so small that the parafrontals of some skeletonized *Aristelliger* remain attached to the remainder of the skull, whereas those of skeletonized *Teratoscincus* do not. Parafrontal bones superficially resemble supraorbital osteoderms. Osteoderms, however, are rare in gekkotans, being present only in *Tarentola*, *Gekko* gecko, and *Geckolepis* (Cartier, 1872; Bauer and Russell, 1989;

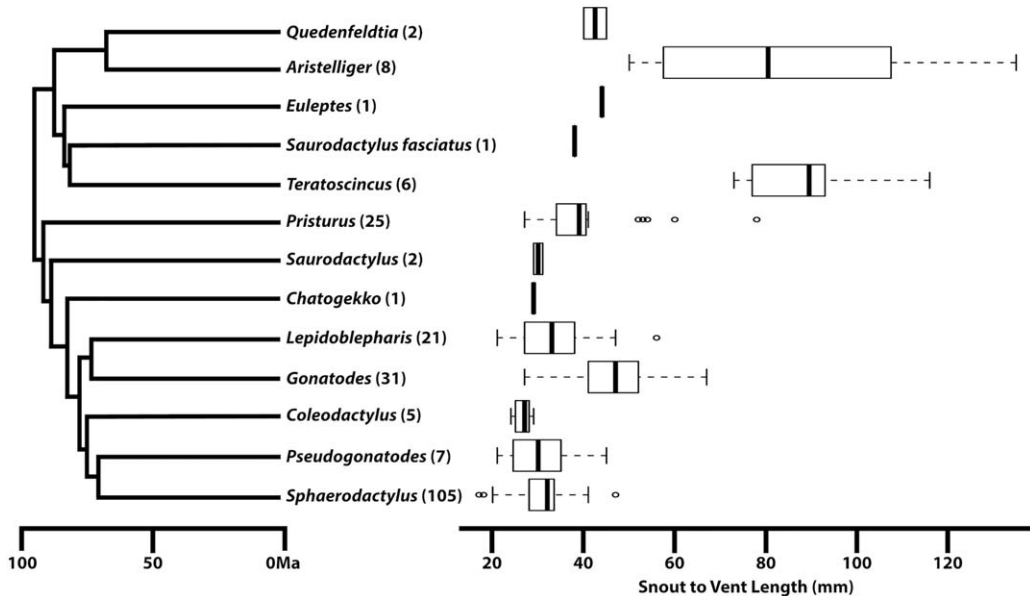


Fig. 1. Chronogram and current molecular hypothesis of the generic relationships within the Sphaerodactylidae (Gamble et al., 2015b). Parenthetical numbers correspond to the recognized number of species within each genus (Uetz, 2017). Adjacent boxplots indicate the range of maximum SVLs for the corresponding genus, based on maximum SVL data for 210 of the 215 recognized sphaerodactylid species (Blanford, 1881; Werner, 1896; Rivero-Blanco, 1968; Hoogmoed, 1973; Thomas, 1975; Schwartz and Henderson, 1991; Avila-Pires, 1995; Schleich et al., 1996; Szczerbak and Golubev, 1996; Anderson, 1999; Hedges and Thomas, 2001; Fong and Diaz, 2004; Barrio-Amorós and Brewer-Carías, 2008; Meiri, 2008; Rivas and Schargel, 2008; Rösler et al., 2008; Díaz and Hedges, 2009; Largen and Spawls, 2010; Rojas-Runjaic et al., 2010; Schargel et al., 2010; Sturaro and Avila-Pires, 2011; Kok, 2011; McCranie and Hedges, 2012; Rivero-Blanco and Schargel, 2012; McCranie and Hedges, 2013; Rivas et al., 2013; Batista et al., 2015; Calderón-Espinosa and Medina-Rangel, 2016; Griffing et al., 2017).

Daza et al., 2015; Vickaryous et al., 2015; Paluh et al., 2017; Scherz et al., 2017). Parafrontal bones lie in the same subdermal plane as the frontal, prefrontal, and postorbitofrontal, suggesting that they are not osteoderms (Bauer and Russell, 1989). Without any obvious evident function, the origin of these enigmatic structures is unknown. Parafrontal bones have not been found in any other squamates and are apparently unique to *Aristelliger* and *Teratoscincus*. However, a supraorbital fibrous sheet, similar to the tissue found dorsal to the parafrontals, has been described in the supraorbital region of the sphaerodactylid *Quedenfeldtia trachyblepharis* (Daza et al., 2008). Because dermal bone partially derives from a mesenchymal matrix (Abzhanov et al., 2007; Vickaryous and Hall, 2008), it is likely that the fibrous sheet is the precursor of parafrontals, which later originate by metaplastic ossification (Levrat-Calviac, 1986, 1987; Levrat-Calviac and Zylberberg, 1986). The presence of this fibrous sheet in *Aristelliger*, *Teratoscincus*, and *Quedenfeldtia* implies a strong likelihood that a similar structure will be present in other members of the same clade (*Sauromactylus fasciatus* and *Euleptes*; Fig. 1). There is only one structure that is comparable in the eublepharid gecko (*Eublepharis macularius*), however, this is a transient element that appears early in the development and becomes fused to the frontal bone (Wise and Russell, 2010). This structure has been interpreted as an anteriorly shifted postfrontal bone, and has not been confirmed in any other gekkotan.

Parafrontal bones were originally observed in *Aristelliger lar* by Hecht (1951), although they remained

unlabeled in the figure in which they were illustrated. In that figure, Hecht illustrated two bony plates of different sizes occupying a supraorbital position, lying in the same plane as the frontal. McDowell and Bogert (1954) noted these elements in Hecht's illustration but mislabeled them collectively as a single palpebral bone, an element present within various groups of the Anguimorpha and Lacertoidea (*sensu* Reeder et al., 2015), but absent from the Gekkota (Evans, 2008; Reeder et al., 2015). Bauer and Russell (1989) subsequently discovered and described parafrontals in both *Teratoscincus scincus* and *A. praesignis*. Based on the hypothesized relationships among gekkotans at the time (Kluge, 1987), these structures were initially regarded as being convergent. Although some topological disagreement exists between current morphological and molecular hypotheses, the most recent phylogenetic hypotheses for sphaerodactylids identify *Aristelliger* and *Teratoscincus* as close relatives, suggesting that their parafrontal bones are homologous (Gamble et al., 2008a; 2008b; 2012; 2015b; Daza and Bauer, 2012). A significant impediment to understanding the evolution of parafrontal bones and assessing their homology is a complete lack of ontogenetic information.

Currently, the presence of parafrontals has only been corroborated for *Aristelliger cochranae*, *A. georgeensis*, *A. lar*, *A. praesignis*, *Teratoscincus bedriagai*, *T. microlepis*, *T. przewalskii*, and *T. scincus* (Bauer and Russell, 1989; Daza et al., 2008). To test the putative homology of parafrontals, we investigated their presence in each representative species of *Aristelliger*, *Teratoscincus*, and all other sphaerodactylid genera. We additionally obtained data from ontogenetic series of *Aristelliger* and *Teratoscincus*

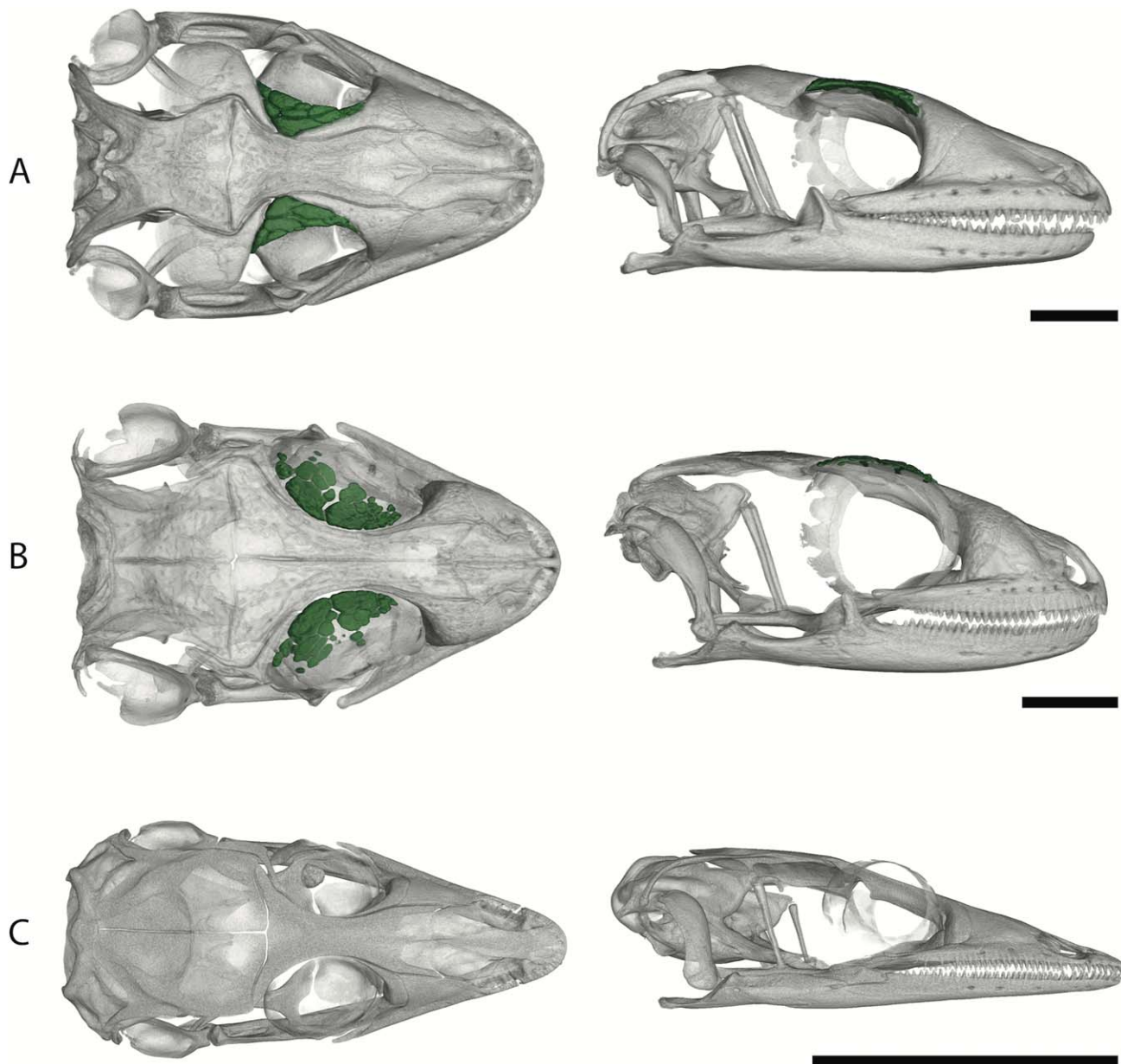


Fig. 2. Dorsal and lateral views of μ CT scans of skulls of (A) *Aristelliger georgeensis* (CAS 176485); (B) *Teratoscincus przewalskii* (CAS 171013); and (C) a sphaerodactyl gecko, *Sphaerodactylus semasiops* (MCZ R-55766). Parafrontal bones are highlighted green. Scale bars = 5 mm.

to determine whether parafrontals in both have the same developmental origins. The close relationship between *Aristelliger* and *Teratoscincus* suggests that their shared expression of parafrontal bones is not the result of convergence, but rather represents homology, at least at some level. That homology may be between the parafrontals themselves, or be associated with an underlying developmental homology that is a necessary precursor to the formation of parafrontals. If the latter prevails, then the actual structures observed in these taxa would be considered to be the result of parallelism (Wake et al., 2011). We hypothesize that the parafrontal bones of *Aristelliger* and *Teratoscincus* are homologous. If homologous,

the presence of these elements exclusively within *Aristelliger* and *Teratoscincus* could be explained by their relatively large body size within the Sphaerodactylidae. Therefore, we hypothesize that there is a threshold body size within this clade of sphaerodactylids, below which parafrontals do not develop, thus explaining their absence in miniaturized taxa.

Our objective is to determine whether the presence of parafrontal bones in *Aristelliger* and *Teratoscincus* is attributable to their phylogenetic relationships, their large body size relative to that of other sphaerodactylids, or the interplay between the two. The enigmatic nature of these elements raises three main questions: (1) are

parafrontals, or a developmental precursor of them, the result of parallel evolution between *Aristelliger* and *Teratoscincus* or is this phenomenon general within this clade or all sphaerodactylids; (2) if parafrontals did not evolve independently, is their presence determined by a threshold size in sphaerodactylids; and finally, (3) is parafrontal expression the result of differential timing in development relative to that of other sphaerodactylids (i.e., heterochrony; Alberch et al., 1979)?

MATERIALS AND METHODS

A total of 279 sphaerodactylid specimens, comprising skeletonized, cleared-and-stained, radiographed, and histologically sectioned preparations, were examined for this study (Tables 1 and 2). The majority of specimens were obtained from institutional collections. A subset of *Teratoscincus keyserlingii* were obtained commercially. A subset of *Aristelliger barbouri* and *A. praesignis* were field-collected on Great Inagua, Bahamas in July of 2015 and Jamaica in June of 2016, respectively. Ontogenetic series of osteological preparations of *Aristelliger* and *Teratoscincus* were examined to investigate gross parafrontal development. A total of 92 individuals of *Aristelliger*, including all described species (except the recently described *A. reyesi*) were examined. A large series of *A. praesignis* was examined to investigate intraspecific variation and the possibility of sexual dimorphism in parafrontal bones. A total of 28 individuals representing six of the seven recognized species of *Teratoscincus* were examined. *Teratoscincus toksunicus* was not included due to its dubious validity. Other sphaerodactylid genera, represented by 69 species (159 total specimens), were examined to serve as morphological comparisons across the spectrum of ontogeny and body size, and to confirm the absence of parafrontal bones in other sphaerodactylid genera. An additional 55 specimens of 38 gekkonan genera were examined for further comparison, composed of representatives of the Carphodactylidae, Diplodactylidae, Eublepharidae, Gekkonidae, and Phyllodactylidae (Table 2). Particular focus of this interfamilial investigation was placed on the genera *Ptenopus* and *Tarentola*, which were studied by Bellairs (1948) and Bauer and Russell (1989) for their atypical supraorbital morphology. All field-collected and commercially obtained individuals were euthanized humanely using a 1% sodium-bicarbonate-buffered tricaine methanesulfonate (MS222) intracoelomic injection and subsequent 50% MS222 intracardiac injection, following the procedure described by Conroy et al. (2009) and under protocols approved by the Villanova University IACUC. Acronyms for institutional collections are: AMB, personal collection of Aaron M. Bauer, Villanova University, PA, USA; AMNH, American Museum of Natural History, New York, NY, USA; AMS, Australian Museum, Sydney, New South Wales, Australia; BMNH, Natural History Museum, London, London, UK; CAS, California Academy of Science, San Francisco, CA, USA; CM, Carnegie Museum of Natural History, Pittsburgh, PA, USA; JVV, collected by Jens Vindum, California Academy of Sciences, San Francisco, CA, USA; KU, University of Kansas Natural History Museum, Lawrence, KS, USA; MCZ, Museum of Comparative Zoology, Harvard University, Cambridge, MA, USA; MVZ, Museum of Vertebrate Zoology, University of California, Berkeley, CA, USA; NMZB,

Natural History Museum, Bulawayo, Zimbabwe; TCWC, Texas Cooperative Wildlife Collection, College Station, TX, USA; UCM, University of Colorado Museum of Natural History, Boulder, CO, USA; USNM and NMNH, National Museum of Natural History, Smithsonian Institution, Washington DC, USA.

Adult and juvenile specimens, obtained in the field and from institutional collections, were skinned and eviscerated using a standard dissection kit. Following a protocol modified from Wassersug (1976) and Hanken and Wassersug (1981), cartilage and bone were stained with alcian blue 8GX and alizarin red S, respectively, and the remaining tissue was subsequently cleared (detailed protocol in Bauer, 1986). Digital radiographs were obtained at the Smithsonian National Museum of Natural History using a KevexTM PXS10-16W X-ray source and Varian Amorphous Silicon Digital X-Ray Detector PaxScan H4030R (130 kV, 81 μ A). The supraorbital region was visualized and imaged using a Nikon SMZ1000 stereomicroscope and Nikon Digital Sight microscope camera. Scale was set by placing a translucent ruler adjacent to cleared and stained specimens or placing a radio-opaque item of a known length adjacent to radiographed specimens. Utilizing the resultant images and additional radiographs, surface area measurements and bony plate counts of osteological preparations were taken using Fiji v2.0.0 (Schindelin et al., 2012). Measurements were rounded to the nearest 0.01 mm² based on the measurements of the smallest total surface area. Only one individual, *A. babouri* (KU 228575), exhibited parafrontal surface area less than 0.01 mm². For several prepared skeletons (e.g., isolated skulls), body size data were unavailable. Because of this, skull lengths (SL) were used as a proxy for SVL. The correlation between SVL and SL is highly significant for the specimens used in this study ($r^2 = 0.9543$, $F = 6122$, $P < 2.2 \times 10^{-16}$; R Core Team, 2014). For comparisons between drastically different sized species, ontogenetic stages are also represented by the percent of total body size (TBS), which was calculated by dividing the individual SVL by the maximum SVL for the particular species.

Preserved juvenile and adult *Aristelliger* and *Teratoscincus* heads were histologically sectioned to compare the morphology of the parafrontals through ontogeny (methods detailed in Supporting Information). Specimen heads and adjacent cervical regions of the spine were removed, dehydrated, and decalcified with Formical-2000 prior to embedding in paraffin wax (Humason, 1979). Decalcification times depended on the size of the specimen. Adequate decalcification was confirmed when a razor blade could be pushed through the exposed cervical vertebrae of the decapitated specimen with minimal resistance. The smallest specimen, *Aristelliger praesignis* (KU 228996; 10.1 mm SL) was successfully decalcified after 20 hr, whereas the largest specimen, *Teratoscincus keyserlingii* (AMB 9211; 22.7 mm SL) was successfully decalcified after 136.5 hr in Formical-2000. Using a rotary microtome, transverse sections were cut 10 μ m thick and subsequently affixed onto glass slides. Slides were stained with Masson's trichrome, following a protocol modified from Garvey (1984; Supporting Information; protocol described in Griffing, 2016). This staining protocol results in nuclei being stained black, collagen green/blue, and muscle fibers and cytoplasm red. All slides were observed and photographed using a Nikon Optiphot compound

TABLE 1. *Aristelliger* and *Teratoscincus* specimens examined in this study

ID	Genus	Species	Prep	SVL (mm)	SL (mm)	Sex	BPC (L)	BPC (R)	Area (L) (mm ²)	Area (R) (mm ²)	TA (mm ²)
<i>Sphaerodactylidae</i>											
AMB 9357	<i>Aristelliger</i>	<i>barbouri</i>	C/S	16.8	5.8		0	0	0.00	0.00	0.00
AMB 9356	<i>Aristelliger</i>	<i>barbouri</i>	C/S	24.4	7.8		0	0	0.00	0.00	0.00
KU 228575	<i>Aristelliger</i>	<i>barbouri</i>	C/S	36.7	10.0	F	2	0	<0.00	<0.00	<0.00
AMB 9354	<i>Aristelliger</i>	<i>barbouri</i>	C/S	38.4	11.0	F	3	3	0.04	0.04	0.08
AMB 9352	<i>Aristelliger</i>	<i>barbouri</i>	C/S	41.6	11.7	F	7	8	0.12	0.14	0.26
AMB 9355	<i>Aristelliger</i>	<i>barbouri</i>	C/S	46.0	12.4	F	1	5	0.23	0.19	0.42
AMNH 45811	<i>Aristelliger</i>	<i>barbouri</i>	C/S	46.0	14.7		3	4	0.35	0.34	0.69
KU 228605	<i>Aristelliger</i>	<i>cochranae</i>	C/S	26.9	8.4		0	0	0.00	0.00	0.00
KU 228603	<i>Aristelliger</i>	<i>cochranae</i>	C/S	41.6	11.9	F	6	4	0.71	0.68	1.39
KU 228597	<i>Aristelliger</i>	<i>cochranae</i>	C/S	46.7	13.1	F	5	5	0.77	0.61	1.38
KU 228585	<i>Aristelliger</i>	<i>cochranae</i>	C/S	58.2	15.6	M	7	9	1.29	1.26	2.55
USNM 305438			R	71.2	20.2		7	8	4.42	4.59	9.01
KU 228722	<i>Aristelliger</i>	<i>expectatus</i>	C/S	17.2	7.0		0	0	0.00	0.00	0.00
KU 228730	<i>Aristelliger</i>	<i>expectatus</i>	C/S	25.5	7.8		0	0	0.00	0.00	0.00
KU 228734	<i>Aristelliger</i>	<i>expectatus</i>	C/S	38.5	10.9		1	2	0.01	0.01	0.02
KU 228702	<i>Aristelliger</i>	<i>expectatus</i>	C/S	41.6	12.7		4	4	0.35	0.34	0.69
AMNH 63014-15			C/S	49.0	15.3	F	9	8	0.77	0.49	1.26
KU 228686	<i>Aristelliger</i>	<i>expectatus</i>	C/S	52.8	14.3	F	14	13	0.83	1.00	1.83
MCZ R 59469	<i>Aristelliger</i>	<i>expectatus</i>	S						0.99	0.78	1.77
UCM 16183	<i>Aristelliger</i>	<i>georgeensis</i>	C/S	33.6	11.6	F	1	0	0.01	0.000	0.01
UCM 16184	<i>Aristelliger</i>	<i>georgeensis</i>	C/S	52.7	15.0	F	5	9	0.65	0.78	1.43
KU 070030	<i>Aristelliger</i>	<i>georgeensis</i>	C/S	78.9	21.5	F	14	11	2.51	2.53	5.05
KU 070036	<i>Aristelliger</i>	<i>georgeensis</i>	C/S	88.1	24.7	M	15	19	5.13	4.74	9.87
KU 070027	<i>Aristelliger</i>	<i>georgeensis</i>	C/S	95.6	25.9	M	14	12	4.57	4.80	9.37
KU 228758	<i>Aristelliger</i>	<i>hechti</i>	C/S	46.4	14.5	F	9	8	0.65	0.52	1.17
KU 228757	<i>Aristelliger</i>	<i>hechti</i>	C/S	86.4	23.1	M	22	21	10.53	10.80	21.33
AMNH 75972	<i>Aristelliger</i>	<i>lar</i>	C/S	31.0	12.5		0	0	0.00	0.00	0.00
KU 228760	<i>Aristelliger</i>	<i>lar</i>	C/S	43.4	14.7		0	0	0.00	0.00	0.00
USNM 260001	<i>Aristelliger</i>	<i>lar</i>	R	49.7	14.2		0	0	0.00	0.00	0.00
KU 228795	<i>Aristelliger</i>	<i>lar</i>	C/S	64.2	19.0		5	4	0.66	0.53	1.19
KU 228792	<i>Aristelliger</i>	<i>lar</i>	C/S	70.9	19.8	F	10	10	1.41	1.40	2.81
USNM 260000	<i>Aristelliger</i>	<i>lar</i>	R	75.6	19.8		7	5	2.40	2.09	4.49
USNM 259999	<i>Aristelliger</i>	<i>lar</i>	R	78.1	19.8		4	4	2.75	3.08	5.83
USNM 259998	<i>Aristelliger</i>	<i>lar</i>	R	80.9	20.5	F	4	6	1.83	2.48	4.31
USNM 041390	<i>Aristelliger</i>	<i>lar</i>	C/S	108.6	24.6	F	20	16	8.82	8.78	17.60
USNM 260004	<i>Aristelliger</i>	<i>lar</i>	R	108.1	24.4	M	9	8	9.29	8.91	18.20
AMNH 46019	<i>Aristelliger</i>	<i>lar</i>	C/S	109.0	25.0		8	8	5.03	5.00	10.03
KU 228785	<i>Aristelliger</i>	<i>lar</i>	C/S	129.9	35.5	M	15	11	18.59	17.76	36.35
MCZ R 63321	<i>Aristelliger</i>	<i>lar</i>	S						9.90	9.65	19.55
MCZ R 194571	<i>Aristelliger</i>	<i>prasignis</i>	C/S	23.0	7.5		0	0	0.00	0.00	0.00
MCZ R 194573	<i>Aristelliger</i>	<i>prasignis</i>	C/S	23.8	8.5		0	0	0.00	0.00	0.00
MCZ R 194563	<i>Aristelliger</i>	<i>prasignis</i>	C/S	28.3	9.6		0	0	0.00	0.00	0.00
KU 228974	<i>Aristelliger</i>	<i>prasignis</i>	C/S	46.2	14.1	F	18	17	1.03	0.99	2.02
MCZ R 194600	<i>Aristelliger</i>	<i>prasignis</i>	C/S	46.4	11.4	M	16	12	0.29	0.30	0.59
NMNH 252332	<i>Aristelliger</i>	<i>prasignis</i>	C/S	46.4	13.4	M	14	22	1.37	1.34	2.71
MCZ R 194590	<i>Aristelliger</i>	<i>prasignis</i>	C/S	52.3	13.0	M	19	22	1.31	1.33	2.64
KU 228978	<i>Aristelliger</i>	<i>prasignis</i>	C/S	52.5	16.6	F	14	10	1.83	1.67	3.50
MCZ R 194574	<i>Aristelliger</i>	<i>prasignis</i>	C/S	52.6	14.5	F	20	22	1.34	1.36	2.70

TABLE 1. (continued).

ID	Genus	Species	Prep	SVL (mm)	SL (mm)	Sex	BPC (L)	Area (L) (mm ²)	Area (R) (mm ²)	TA (mm ²)
NMMNH 192525	Aristelliger	<i>praesignis</i>	C/S	52.8	15.2	F	27	1.87	1.79	3.66
MCZ R 194567	Aristelliger	<i>praesignis</i>	C/S	54.0	15.7	F	15	1.28	1.02	2.30
MCZ R 194581	Aristelliger	<i>praesignis</i>	C/S	57.9	16.7	M	22	15	2.23	2.11
MCZ R 194582	Aristelliger	<i>praesignis</i>	C/S	58.1	15.2	F	31	31	1.36	4.34
MVZ 69636	Aristelliger	<i>praesignis</i>	C/S	59.0	16.8	F	23	20	2.91	1.44
MCZ R 194566	Aristelliger	<i>praesignis</i>	C/S	60.3	16.2	M	19	20	1.78	3.35
MCZ R 194565	Aristelliger	<i>praesignis</i>	C/S	60.7	16.8	F	13	15	2.26	1.85
MCZ R 194587	Aristelliger	<i>praesignis</i>	C/S	60.8	17.6	F	21	18	1.94	2.06
MCZ R 194588	Aristelliger	<i>praesignis</i>	C/S	60.8	17.8	M	19	17	1.72	1.79
AMNH 146747	Aristelliger	<i>praesignis</i>	C/S	61.0	20.3	F	8	6	1.20	1.52
AMNH 146748	Aristelliger	<i>praesignis</i>	C/S	64.0	18.5	F	6	2	0.75	0.28
MCZ R 194577	Aristelliger	<i>praesignis</i>	C/S	64.8	17.0	F	23	23	2.94	2.65
MCZ R 194599	Aristelliger	<i>praesignis</i>	C/S	64.9	17.9	F	30	24	3.16	2.99
MCZ R 194585	Aristelliger	<i>praesignis</i>	C/S	67.3	18.0	F	15	13	2.35	2.04
NMMNH 252333	Aristelliger	<i>praesignis</i>	C/S	67.5	18.6	F	37	34	3.14	3.35
MCZ R 194568	Aristelliger	<i>praesignis</i>	C/S	68.1	18.1	F	18	19	3.70	3.30
MCZ R 194580	Aristelliger	<i>praesignis</i>	C/S	69.7	17.2	F	11	14	3.11	3.06
MCZ R 194596	Aristelliger	<i>praesignis</i>	C/S	71.2	18.6	F	6	9	3.06	2.86
MCZ R 194575	Aristelliger	<i>praesignis</i>	C/S	74.9	19.7	M	10	14	2.50	2.55
MCZ R 194583	Aristelliger	<i>praesignis</i>	C/S	74.9	20.3	M	9	8	3.48	3.25
AMNH 75976	Aristelliger	<i>praesignis</i>	C/S	75.0	23.3	M	23	27	4.69	4.20
USNMN 494664	Aristelliger	<i>praesignis</i>	R	78.0	20.0	M	27	7	2.73	4.18
MCZ R 194578	Aristelliger	<i>praesignis</i>	C/S	78.54	21.0	M	20	22	5.13	5.08
MCZ R 194579	Aristelliger	<i>praesignis</i>	C/S	83.2	21.2	M	20	22	5.53	5.14
MCZ R 194584	Aristelliger	<i>praesignis</i>	C/S	83.5	20.6	M	7	9	3.67	3.85
MCZ R 194576	Aristelliger	<i>praesignis</i>	C/S	86.5	21.5	M	16	17	4.49	4.53
KU 228995	Aristelliger	<i>praesignis</i>	C/S	87.5	23.6	M	13	14	5.82	4.83
MCZ R 194595	Aristelliger	<i>praesignis</i>	C/S	88.2	21.9	M	8	8	6.03	5.83
MCZ R 194597	Aristelliger	<i>praesignis</i>	C/S	88.3	21.9	M	9	9	7.36	7.73
MCZ R 194591	Aristelliger	<i>praesignis</i>	C/S	89.6	23.1	M	20	20	5.24	4.77
MCZ R 194596	Aristelliger	<i>praesignis</i>	C/S	93.4	24.6	M	36	38	8.11	7.73
MCZ R 194593	Aristelliger	<i>praesignis</i>	C/S	96.6	24.9	M	28	40	10.07	9.26
MCZ R 194592	Aristelliger	<i>praesignis</i>	C/S	96.9	23.8	M	20	20	7.62	6.67
MCZ R 194591	Aristelliger	<i>praesignis</i>	C/S	97.5	25.3	M	26	22	10.07	8.46
MCZ R 194594	Aristelliger	<i>praesignis</i>	C/S	98.0	24.7	M	18	16	7.06	6.51
AMNH 71595	Aristelliger	<i>praesignis</i>	S	18.2	36	S	26	38	3.87	3.94
BMNH 1964.1812	Aristelliger	<i>praesignis</i>	S	18.3	36	S	21	23	3.46	3.11
CAS 39359	Aristelliger	<i>praesignis</i>	S	19.3	25	S	23	23	4.13	3.64
AMNH 71594	Aristelliger	<i>praesignis</i>	S	19.5	5	S	24	24	1.45	1.49
MCZ R 7342	Aristelliger	<i>praesignis</i>	S	20.4	3	S	27	27	7.28	6.90
MCZ R 9606	Aristelliger	<i>praesignis</i>	S	21.6	10.1	F	8	8	1.98	1.45
KU 228996	Aristelliger	<i>praesignis</i>	H	29.9	45.46	F	7	7	0	0.00
No Data	Aristelliger	<i>praesignis</i>	H	37.4	12.0	F	0	0	0.00	0.00
CAS 167421	Teratoscincus	<i>przewalskii</i>	C/S	82.5	20.3	F	29	29	6.30	6.08
CAS 167393	Teratoscincus	<i>przewalskii</i>	C/S	82.5	21.1	F	19	19	5.67	5.65
CAS 167394	Teratoscincus	<i>przewalskii</i>	C/S	84.4	22.3	M	15	15	6.44	5.91
CAS 167390	Teratoscincus	<i>przewalskii</i>	C/S	85.5	22.6	M	17	17	11.45	12.95

TABLE 1. (continued).

ID	Genus	Species	Prep	SVL (mm)	SL (mm)	Sex	BPC (L)	BPC (R)	Area (L) (mm ²)	Area (R) (mm ²)	TA (mm ²)
MVZ 236999	<i>Teratoscincus</i>	<i>bedriagai</i>	C/S	56.2	14.2	M	32	24	3.38	3.19	6.57
MVZ 237000	<i>Teratoscincus</i>	<i>bedriagai</i>	C/S	60.0	16.3	M	32	32	5.32	5.52	10.84
MVZ 237001	<i>Teratoscincus</i>	<i>bedriagai</i>	C/S	62.3	17.3	M	43	47	5.63	5.85	11.48
MVZ 237002	<i>Teratoscincus</i>	<i>bedriagai</i>	C/S	63.4	16.9	M	30	37	6.39	6.64	13.03
CAS 228581	<i>Teratoscincus</i>	<i>bedriagai</i>	C/S	65.4	17.8	M	35	35	6.57	6.96	13.53
MVZ 208967	<i>Teratoscincus</i>	<i>boroworskii</i>	C/S	44.2	14.0	F	10	7	0.27	0.25	0.52
CAS 168088	<i>Teratoscincus</i>	<i>boroworskii</i>	C/S	48.5	14.5	F	26	27	0.37	0.38	0.75
MVZ 208966	<i>Teratoscincus</i>	<i>boroworskii</i>	C/S	60.6	17.6	F	16	17	2.00	2.06	4.06
MVZ 208965	<i>Teratoscincus</i>	<i>boroworskii</i>	C/S	69.3	18.9	M	58	57	9.21	10.12	19.33
CAS 168055	<i>Teratoscincus</i>	<i>boroworskii</i>	C/S	86.0	24.7	F	39	37	13.91	14.69	28.60
CAS 199550	<i>Teratoscincus</i>	<i>scincus</i>	C/S	42.0	11.7	F	0	0	0.00	0.00	0.00
AMB 1237	<i>Teratoscincus</i>	<i>scincus</i>	C/S	64.0	18.9	F	19	15	7.18	6.60	13.78
AMB 1238	<i>Teratoscincus</i>	<i>scincus</i>	C/S	65.5	19.6	F	37	31	9.19	9.40	18.59
CAS 179125	<i>Teratoscincus</i>	<i>scincus</i>	C/S	85.3	23.3	F	28	25	18.36	19.64	38.00
CAS 101437	<i>Teratoscincus</i>	<i>scincus</i>	C/S	97.0	25.8	F	40	33	25.82	25.82	51.64
MVZ 243568	<i>Teratoscincus</i>	<i>microlepis</i>	C/S	43.3	19.1	M	22	20	10.15	10.68	20.83
CAS 228807	<i>Teratoscincus</i>	<i>keyserlingii</i>	C/S	84.6	22.5	M	26	28	17.68	17.66	35.34
CAS 167423	<i>Teratoscincus</i>	<i>przewalskii</i>	H	37.6	12.6						
CAS 168087	<i>Teratoscincus</i>	<i>roborowskii</i>	H	51.5	16.3						
CAS 199551	<i>Teratoscincus</i>	<i>scincus</i>	H	41.7							
No Data	<i>Teratoscincus</i>	<i>keyserlingii</i>	H	56.5	17.2	M					
AMB 9210	<i>Teratoscincus</i>	<i>keyserlingii</i>	H	91.1	22.7	M					
AMB 9211	<i>Teratoscincus</i>	<i>keyserlingii</i>	H								

Preparations include cleared-and-stained (C/S), radiographs (R), skeletonized (S), or histological sections (H). Measurements are snout-to-vent length (SVL), skull length (SL), bony plate counts of both left (BPC[L]) and right (BPC[R]) sides, bony plate surface areas of both left (Area [L]) and right (Area [R]) sides, and total bony plate surface area (TA). Empty cells indicate the data are unknown (e.g., skeletonized specimen that does not have SVL measurements).

TABLE 2. Specimens other than *Aristelliger* and *Teratoscincus* examined in this study

ID	Genus	Species	Prep	SVL (mm)	SL (mm)
<i>Sphaerodactylidae</i>					
AMNH 138670	<i>Chatogekko</i>	<i>amazonicus</i>	C/S	21.0	4.8
AMNH 132052	<i>Chatogekko</i>	<i>amazonicus</i>	C/S	23.0	5.2
USNM 200663	<i>Chatogekko</i>	<i>amazonicus</i>	R	14.7	4.7
USNM 288765	<i>Chatogekko</i>	<i>amazonicus</i>	R	16.6	4.7
USNM 288763	<i>Chatogekko</i>	<i>amazonicus</i>	R	22.1	5.0
USNM 303472	<i>Chatogekko</i>	<i>amazonicus</i>	R	20.1	5.4
USNM 303473	<i>Chatogekko</i>	<i>amazonicus</i>	R	20.7	5.0
USNM 288776	<i>Chatogekko</i>	<i>amazonicus</i>	R	20.9	5.4
USNM 288775	<i>Chatogekko</i>	<i>amazonicus</i>	R	20.6	5.2
USNM 288788	<i>Chatogekko</i>	<i>amazonicus</i>	R	18.9	5.3
USNM 288766	<i>Chatogekko</i>	<i>amazonicus</i>	R	18.5	4.8
USNM 288771	<i>Chatogekko</i>	<i>amazonicus</i>	R	20.5	5.2
USNM 288785	<i>Chatogekko</i>	<i>amazonicus</i>	R	21.2	5.0
USNM 288777	<i>Chatogekko</i>	<i>amazonicus</i>	R	21.5	5.2
USNM 288786	<i>Chatogekko</i>	<i>amazonicus</i>	R	22.0	5.9
USNM 288782	<i>Chatogekko</i>	<i>amazonicus</i>	R	20.2	6.1
USNM 288787	<i>Chatogekko</i>	<i>amazonicus</i>	R	20.7	5.2
USNM 288778	<i>Chatogekko</i>	<i>amazonicus</i>	R	20.0	4.7
USNM 288767	<i>Chatogekko</i>	<i>amazonicus</i>	R	18.0	4.7
USNM 288769	<i>Chatogekko</i>	<i>amazonicus</i>	R	21.3	5.9
USNM 288770	<i>Chatogekko</i>	<i>amazonicus</i>	R	20.5	5.3
USNM 288781	<i>Chatogekko</i>	<i>amazonicus</i>	R	18.7	4.9
USNM 289066	<i>Chatogekko</i>	<i>amazonicus</i>	R	17.6	5.0
USNM 289063	<i>Chatogekko</i>	<i>amazonicus</i>	R	18.8	4.8
USNM 289062	<i>Chatogekko</i>	<i>amazonicus</i>	R	21.1	5.0
USNM 304122	<i>Coleodactylus</i>	<i>guimaraesi</i>	R	20.6	5.3
USNM 566300	<i>Coleodactylus</i>	<i>septentrionalis</i>	R	20.4	5.2
USNM 302285	<i>Coleodactylus</i>	<i>septentrionalis</i>	R	26.8	6.4
USNM 302286	<i>Coleodactylus</i>	<i>septentrionalis</i>	R	14.2	4.9
USNM 302287	<i>Coleodactylus</i>	<i>septentrionalis</i>	R	15.0	4.5
USNM 531621	<i>Coleodactylus</i>	<i>septentrionalis</i>	R	22.2	6.6
USNM 531622	<i>Coleodactylus</i>	<i>septentrionalis</i>	R	25.7	6.6
USNM 302348	<i>Coleodactylus</i>	<i>septentrionalis</i>	R	27.9	6.3
USNM 302338	<i>Coleodactylus</i>	<i>septentrionalis</i>	R	17.3	5.1
USNM 302350	<i>Coleodactylus</i>	<i>septentrionalis</i>	R	25.9	6.0
USNM 302354	<i>Coleodactylus</i>	<i>septentrionalis</i>	R	27.0	6.5
USNM 302351	<i>Coleodactylus</i>	<i>septentrionalis</i>	R	22.8	5.9
USNM 302337	<i>Coleodactylus</i>	<i>septentrionalis</i>	R	28.1	6.4
USNM 302361	<i>Coleodactylus</i>	<i>septentrionalis</i>	R	25.0	6.5
USNM 302355	<i>Coleodactylus</i>	<i>septentrionalis</i>	R	21.3	5.4
USNM 302345	<i>Coleodactylus</i>	<i>septentrionalis</i>	R	15.8	4.9
USNM 302342	<i>Coleodactylus</i>	<i>septentrionalis</i>	R	24.0	6.2
USNM 302356	<i>Coleodactylus</i>	<i>septentrionalis</i>	R	21.2	5.7
USNM 302340	<i>Coleodactylus</i>	<i>septentrionalis</i>	R	25.6	6.2
USNM 302343	<i>Coleodactylus</i>	<i>septentrionalis</i>	R	16.4	4.8
USNM 302358	<i>Coleodactylus</i>	<i>septentrionalis</i>	R	22.1	5.7
USNM 302344	<i>Coleodactylus</i>	<i>septentrionalis</i>	R	16.9	5.1
USNM 302349	<i>Coleodactylus</i>	<i>septentrionalis</i>	R	27.1	6.5
AMNH 144404	<i>Euleptes</i>	<i>europea</i>	C/S	30.0	10.2
TCWC 78071	<i>Euleptes</i>	<i>europea</i>	C/S	35.5	9.8
USNM 014861	<i>Euleptes</i>	<i>europea</i>	R	41.2	12.2
NMNH 58963	<i>Euleptes</i>	<i>europea</i>	C/S	37.5	11.2
AMNH 144393	<i>Gonatodes</i>	<i>atricucullaris</i>	C/S	28.0	6.4
AMNH 146764	<i>Gonatodes</i>	<i>atricucullaris</i>	C/S	31.0	8.7
AMNH 108712	<i>Gonatodes</i>	<i>ceciliae</i>	C/S	49.1	14.0
NMNH 349540	<i>Gonatodes</i>	<i>ceciliae</i>	H		
NMNH 349541	<i>Gonatodes</i>	<i>ceciliae</i>	H		
NMNH 349542	<i>Gonatodes</i>	<i>ceciliae</i>	H		
MVZ 83412	<i>Gonatodes</i>	sp.	C/S	18.0	5.5
MVZ 83402	<i>Gonatodes</i>	<i>albogularis</i>	C/S	36.7	9.2
MVZ 83369	<i>Gonatodes</i>	<i>albogularis</i>	C/S	37.5	10.2
USNM 297802	<i>Gonatodes</i>	<i>albogularis</i>	R	40.3	8.5
USNM 535791	<i>Gonatodes</i>	<i>annularis</i>	R	43.8	11.5
USNM 535787	<i>Gonatodes</i>	<i>annularis</i>	R	36.2	10.4
USNM 94980	<i>Gonatodes</i>	<i>antillensis</i>	R	30.1	8.4
USNM 568677	<i>Gonatodes</i>	<i>humeralis</i>	R	37.6	9.7

TABLE 2. (continued).

ID	Genus	Species	Prep	SVL (mm)	SL (mm)
USNM 568692	<i>Gonatodes</i>	<i>humeralis</i>	R	37.9	11.0
USNM 568645	<i>Gonatodes</i>	<i>humeralis</i>	R	37.3	10.6
USNM 568681	<i>Gonatodes</i>	<i>humeralis</i>	R	39.8	10.8
USNM 568663	<i>Gonatodes</i>	<i>humeralis</i>	R	37.1	10.4
USNM 568684	<i>Gonatodes</i>	<i>humeralis</i>	R	35.3	8.9
USNM 568647	<i>Gonatodes</i>	<i>humeralis</i>	R	37.1	10.0
USNM 568658	<i>Gonatodes</i>	<i>humeralis</i>	R	31.6	9.1
AMNH 144541	<i>Lepidoblepharis</i>	<i>xanthostigma</i>	C/S	35.0	7.1
MVZ 77215	<i>Lepidoblepharis</i>	<i>perraccae</i>	C/S	21.6	6.2
USNM 234565	<i>Lepidoblepharis</i>	<i>buchwaldi</i>	R	28.2	6.7
USNM 234566	<i>Lepidoblepharis</i>	<i>buchwaldi</i>	R	28.6	7.1
USNM 166142	<i>Lepidoblepharis</i>	<i>festae</i>	R	30.9	7.2
USNM 166141	<i>Lepidoblepharis</i>	<i>festae</i>	R	28.2	7.3
USNM 166143	<i>Lepidoblepharis</i>	<i>festae</i>	R	20.7	5.8
USNM 217635	<i>Lepidoblepharis</i>	<i>heyerorum</i>	R	30.2	6.4
AMNH 20032	<i>Pristurus</i>	sp.	C/S	29.0	7.7
AMNH 20056	<i>Pristurus</i>	sp.	C/S	36.0	9.5
MCZ R 157119	<i>Pristurus</i>	<i>carteri</i>	C/S	69.0	16.7
USNM 72014	<i>Pristurus</i>	<i>crucifer</i>	R	35.0	8.6
USNM 217452	<i>Pristurus</i>	<i>crucifer</i>	R	33.3	8.1
USNM 217453	<i>Pristurus</i>	<i>crucifer</i>	R	34.1	9.2
AMNH 146746	<i>Pseudogonatodes</i>	<i>barbouri</i>	C/S	21.0	5.2
USNM 333018	<i>Pseudogonatodes</i>	<i>guianensis</i>	R	22.6	5.8
USNM 538263	<i>Pseudogonatodes</i>	<i>guianensis</i>	R	27.0	6.2
USNM 538264	<i>Pseudogonatodes</i>	<i>guianensis</i>	R	24.6	6.0
USNM 538260	<i>Pseudogonatodes</i>	<i>guianensis</i>	R	27.0	6.5
USNM 538261	<i>Pseudogonatodes</i>	<i>guianensis</i>	R	22.4	6.4
USNM 538574	<i>Pseudogonatodes</i>	<i>guianensis</i>	R	22.4	5.5
USNM 566327	<i>Pseudogonatodes</i>	<i>guianensis</i>	R	28.2	6.9
USNM 343190	<i>Pseudogonatodes</i>	<i>peruvianus</i>	R	24.0	6.1
CM 55055A	<i>Quedenfeldtia</i>	<i>trachyblepharus</i>	C/S	43.6	11.7
MVZ 178124	<i>Quedenfeldtia</i>	<i>trachyblepharus</i>	C/S	43.5	11.1
USNM 196417	<i>Quedenfeldtia</i>	<i>trachyblepharus</i>	R	40.3	10.4
MVZ 162547	<i>Saurodactylus</i>	<i>fasciatus</i>	C/S	18.3	6.8
USNM 217454	<i>Saurodactylus</i>	<i>mauritanicus</i>	R	27.7	7.4
MVZ 149093	<i>Sphaerodactylus</i>	<i>glaucus</i>	C/S	25.2	6.6
MVZ 149088	<i>Sphaerodactylus</i>	<i>glaucus</i>	C/S	26.7	7.2
USNM 541810	<i>Sphaerodactylus</i>	<i>ariasae</i>	R	13.7	4.1
USNM 541809	<i>Sphaerodactylus</i>	<i>ariasae</i>	R	15.0	4.2
USNM 260054	<i>Sphaerodactylus</i>	<i>armstrongi</i>	R	22.9	6.1
USNM 260052	<i>Sphaerodactylus</i>	<i>armstrongi</i>	R	21.9	6.1
USNM 260046	<i>Sphaerodactylus</i>	<i>armstrongi</i>	R	21.8	5.7
USNM 328949	<i>Sphaerodactylus</i>	<i>asterulus</i>	R	25.2	6.5
USNM 304481	<i>Sphaerodactylus</i>	<i>beatyi</i>	R	24.2	6.7
USNM 292296	<i>Sphaerodactylus</i>	<i>cinereus</i>	R	29.2	8.2
USNM 118881	<i>Sphaerodactylus</i>	<i>copei</i>	R	30.9	8.9
USNM 211428	<i>Sphaerodactylus</i>	<i>corticola</i>	R	28.5	8.3
USNM 328962	<i>Sphaerodactylus</i>	<i>darlingtoni</i>	R	21.8	6.4
USNM 328965	<i>Sphaerodactylus</i>	<i>difficilis</i>	R	28.8	8.2
USNM 27625	<i>Sphaerodactylus</i>	<i>elegans</i>	R	39.7	10.6
USNM 512253	<i>Sphaerodactylus</i>	<i>ladae</i>	R	28.9	7.3
USNM 197338	<i>Sphaerodactylus</i>	<i>leucaster</i>	R	26.0	6.9
USNM 220921	<i>Sphaerodactylus</i>	<i>levinsi</i>	R	29.7	7.7
USNM 120503	<i>Sphaerodactylus</i>	<i>lineolatus</i>	R	27.8	8.4
USNM 120479	<i>Sphaerodactylus</i>	<i>lineolatus</i>	R	27.7	7.8
USNM 221462	<i>Sphaerodactylus</i>	<i>macrolepis</i>	R	23.0	5.8
USNM 494822	<i>Sphaerodactylus</i>	<i>notatus</i>	R	24.7	6.4
AMNH 73470	<i>Sphaerodactylus</i>	<i>nigropunctatus</i>	C/S	26.0	6.7
USNM 157532	<i>Sphaerodactylus</i>	<i>pacificus</i>	R	37.1	9.4
USNM 309772	<i>Sphaerodactylus</i>	<i>ramsdeni</i>	R	31.5	7.8
USNM 326996	<i>Sphaerodactylus</i>	<i>roosevelti</i>	R	34.8	9.2
USNM 327042	<i>Sphaerodactylus</i>	<i>roosevelti</i>	R	34.8	8.9
USNM 326986	<i>Sphaerodactylus</i>	<i>roosevelti</i>	R	35.7	10.0
USNM 326987	<i>Sphaerodactylus</i>	<i>roosevelti</i>	R	35.0	9.7
USNM 78921	<i>Sphaerodactylus</i>	<i>ruibali</i>	R	29.7	8.9
USNM 260157	<i>Sphaerodactylus</i>	<i>savagei</i>	R	28.8	6.8
USNM 252126	<i>Sphaerodactylus</i>	<i>richardsoni</i>	R	39.0	10.5

TABLE 2. (continued).

ID	Genus	Species	Prep	SVL (mm)	SL (mm)
USNM 222901	<i>Sphaerodactylus</i>	<i>microlepis</i>	R	31.7	8.4
USNM 140431	<i>Sphaerodactylus</i>	<i>oliveri</i>	R	29.1	8.3
USNM 328281	<i>Sphaerodactylus</i>	<i>parkeri</i>	R	33.9	10.2
USNM 305428	<i>Sphaerodactylus</i>	<i>randi</i>	R		6.8
USNM 236098	<i>Sphaerodactylus</i>	<i>sabanus</i>	R	26.4	6.8
USNM 305435	<i>Sphaerodactylus</i>	<i>semasiops</i>	R	24.6	7.4
USNM 292294	<i>Sphaerodactylus</i>	<i>semasiops</i>	R	28.8	8.1
USNM 570209	<i>Sphaerodactylus</i>	<i>rosaura</i>	R	35.3	9.2
USNM 570196	<i>Sphaerodactylus</i>	<i>rosaura</i>	R	38.0	9.8
USNM 570208	<i>Sphaerodactylus</i>	<i>rosaura</i>	R	37.6	10.0
USNM 570198	<i>Sphaerodactylus</i>	<i>rosaura</i>	R	35.5	9.3
USNM 570207	<i>Sphaerodactylus</i>	<i>rosaura</i>	R	37.7	10.9
USNM 570206	<i>Sphaerodactylus</i>	<i>rosaura</i>	R	39.0	10.5
USNM 570199	<i>Sphaerodactylus</i>	<i>rosaura</i>	R	37.0	10.2
USNM 229891	<i>Sphaerodactylus</i>	<i>micropithecus</i>	R	34.1	9.5
USNM 292289	<i>Sphaerodactylus</i>	<i>oxyrhinus</i>	R	32.6	9.4
USNM 292288	<i>Sphaerodactylus</i>	<i>oxyrhinus</i>	R	31.1	9.1
USNM 221593	<i>Sphaerodactylus</i>	<i>parthenopion</i>	R	17.0	4.9
USNM 292328	<i>Sphaerodactylus</i>	<i>rhabdotus</i>	R	27.5	7.9
USNM 319135	<i>Sphaerodactylus</i>	<i>samanensis</i>	R	27.3	7.4
USNM 292313	<i>Sphaerodactylus</i>	<i>sammeri</i>	R	32.1	8.7
USNM 236118	<i>Sphaerodactylus</i>	<i>sputator</i>	R	30.7	8.3
USNM 140270	<i>Sphaerodactylus</i>	<i>torrei</i>	R	34.6	8.5
USNM 291193	<i>Sphaerodactylus</i>	<i>townsendi</i>	R	20.5	5.9
USNM 328977	<i>Sphaerodactylus</i>	<i>thompsoni</i>	R	29.6	7.7
USNM 286941	<i>Sphaerodactylus</i>	<i>vincenti</i>	R	32.2	8.3
<i>Phyllodactylidae</i>					
MVZ 188639	<i>Homonota</i>	<i>darwini</i>	C/S	48.0	11.5
AMB 1455	<i>Tarentola</i>	<i>chazaliae</i>	C/S	60.2	19.6
MVZ 178184	<i>Tarentola</i>	<i>mauritanica</i>	C/S	65.3	19.0
CAS 91351	<i>Phyllodactylus</i>	<i>unctus</i>	C/S	50.0	13.6
MVZ 97495	<i>Ptyodactylus</i>	<i>hasselquistii</i>	C/S	74.7	21.8
MVZ 174998	<i>Thecadactylus</i>	<i>rapicauda</i>	C/S	86.7	23.0
<i>Eublepharidae</i>					
MVZ 111777	<i>Aleuroscalobotes</i>	<i>felinus</i>	C/S	82.6	22.8
AMB 1767	<i>Coleonyx</i>	<i>elegans</i>	C/S	90.0	20.0
<i>Carphodactylidae</i>					
AMB 48	<i>Nephrurus</i>	<i>deleani</i>	C/S	73.2	13.5
No Data	<i>Phyllurus</i>	<i>platurus</i>	C/S	40.9	13.5
<i>Diplodactylidae</i>					
AMS R 78350	<i>Bavayia</i>	<i>sauvagii</i>	C/S	62.0	15.6
AMS R 78351	<i>Bavayia</i>	<i>sauvagii</i>	C/S	53.0	14.7
MVZ 81625	<i>Strophurus</i>	<i>elderi</i>	C/S	44.3	11.9
AMB 89	<i>Woodworthia</i>	<i>maculata</i>	C/S	30.9	10.2
AMB 90	<i>Woodworthia</i>	<i>maculata</i>	C/S	60.2	15.9
AMB 54	<i>Lucasium</i>	<i>damaeum</i>	C/S	53.7	14.1
AMB 1766	<i>Naultinus</i>	<i>grayii</i>	C/S	80.0	20.8
AMB 1765	<i>Pseudothecadactylus</i>	<i>lindneri</i>	C/S	99.5	29.9
CAS 165898	<i>Rhacodactylus</i>	<i>auriculatus</i>	C/S	111.0	32.5
<i>Gekkonidae</i>					
CAS 126206	<i>Afroedura</i>	<i>africana</i>	C/S	54.6	15.2
CAS 8421	<i>Ailuronyx</i>	<i>seychellensis</i>	C/S	73.3	20.0
CAS 140599	<i>Bunopus</i>	<i>crassicauda</i>	C/S	47.6	13.6
CAS 8644	<i>Chondrodactylus</i>	<i>angulifer</i>	C/S	102.2	26.7
AMB 3061	<i>Chondrodactylus</i>	<i>bibronii</i>	C/S	71.2	20.8
CAS H8578	<i>Chondrodactylus</i>	<i>bibronii</i>	C/S	61.8	18.4
CAS H8679	<i>Chondrodactylus</i>	<i>bibronii</i>	C/S	55.8	16.8
MVZ 75465	<i>Cnemaspis</i>	<i>spinicollis</i>	C/S	44.2	12.4
MVZ 111784	<i>Cyrtodactylus</i>	<i>malayanus</i>	C/S	99.9	24.7
No Data	<i>Gekko</i>	<i>gecko</i>	C/S	104.3	28.0
CAS 156884	<i>Geckolepis</i>	<i>maculatus</i>	C/S	67.8	14.7
MVZ 705247	<i>Gehyra</i>	<i>mutilata</i>	C/S	72.4	20.1
AMB 2438	<i>Goggia</i>	<i>microlepidota</i>	C/S	67.0	16.2
MVZ 75492	<i>Hemidactylus</i>	<i>brookii</i>	C/S	59.0	15.7
MCZ A27237	<i>Hemidactylus</i>	<i>mabouia</i>	C/S	56.8	15.1
CAS 145927	<i>Hemiphyllodactylus</i>	<i>typus</i>	C/S	34.6	8.1
NMZB 13693	<i>Homopholis</i>	<i>wahlbergii</i>	C/S	87.7	21.3

TABLE 2. (continued).

ID	Genus	Species	Prep	SVL (mm)	SL (mm)
MVZ 75471	<i>Lygodactylus</i>	<i>conruai</i>	C/S	25.0	7.5
CAS 186290	<i>Narudasia</i>	<i>festiva</i>	C/S	28.5	8.5
AMB 2279	<i>Pachydactylus</i>	<i>maculatus</i>	C/S	37.1	10.6
AMB 2274	<i>Pachydactylus</i>	<i>maculatus</i>	C/S	36.8	9.8
CAS 195506	<i>Pachydactylus</i>	<i>vansoni</i>	C/S	48.5	13.6
CAS 159768	<i>Perochirus</i>	<i>ateles</i>	C/S	60.1	17.7
CAS-SUR 13961	<i>Phelsuma</i>	<i>madagascariensis</i>	C/S	78.2	20.7
AMB 8444	<i>Phelsuma</i>	<i>astriata</i>	C/S	52.6	14.2
CAS 126295	<i>Phelsuma</i>	<i>quadriocellata</i>	C/S	51.2	14.0
AMB 8435	<i>Phelsuma</i>	<i>sundbergi</i>	C/S	75.5	17.8
CAS 128978	<i>Pseudogekko</i>	<i>brevipes</i>	C/S	49.0	12.9
CAS 8640	<i>Ptenopus</i>	<i>garrulus</i>	C/S	56.3	13.9
CAS 8657	<i>Ptenopus</i>	<i>garrulus</i>	C/S	39.2	10.6
CAS 8641	<i>Ptenopus</i>	<i>garrulus</i>	C/S	54.3	13.4
JVV 1781	<i>Rhoptropus</i>	<i>biporusus</i>	C/S	44.8	12.1
JVV 1743	<i>Rhoptropus</i>	<i>biporusus</i>	C/S	35.8	11.0
AMB 4021	<i>Rhoptropus</i>	<i>boultoni</i>	C/S	53.8	15.0
JVV 1659	<i>Rhoptropus</i>	<i>boultoni</i>	C/S	62.4	17.0
CAS 134640	<i>Stenodactylus</i>	<i>petrii</i>	C/S	58.8	15.7

Preparations include cleared-and-stained (C/S), radiographs (R), skeletonized (S), or histological sections (H). Measurements are snout-to-vent length (SVL) and skull length (SL). Empty cells indicate the data are unknown (e.g., skeletonized specimen that does not have SVL measurements).

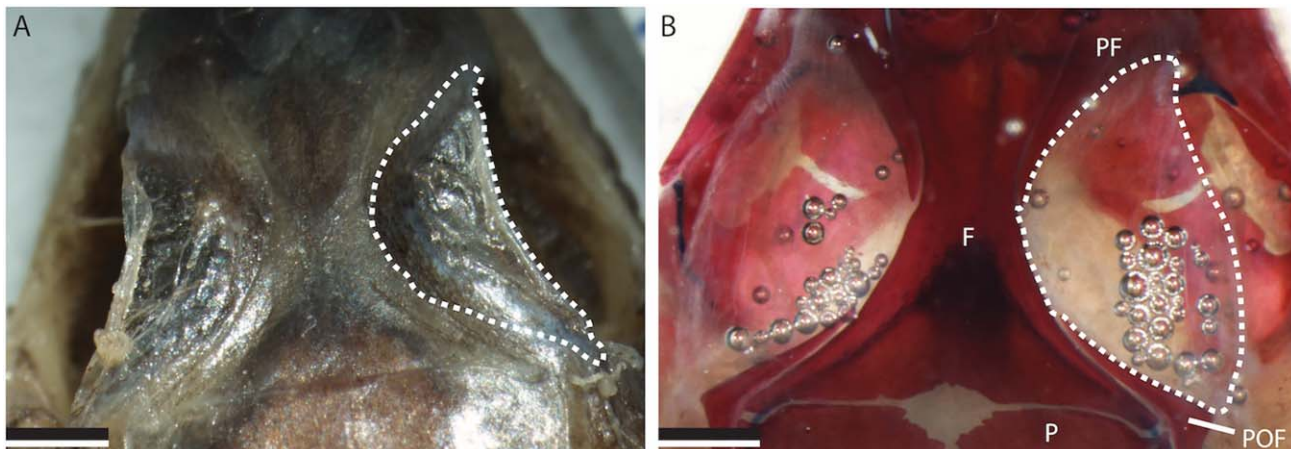


Fig. 3. Dorsal view of the frontal region of a skinned (A) and subsequently cleared-and-stained (B) *Quedenfeldtia trachyblepharus* (CM 55055A) exhibiting supraorbital fibrous sheets in the extra-brillar fringe (dashed lines). F, frontal; P, parietal; PF, prefrontal; POF, postorbitofrontal. Scale bars = 1 mm.

microscope and Nikon Digital Sight microscope camera. Tissues adjacent to the parafrontals were noted.

RESULTS

Presence of Parafrontal Bones and Supraorbital Skeletogenic Fibrous Sheets in the Sphaerodactylidae

We verified the presence of parafrontal bones in all examined species of *Aristelliger* and *Teratoscincus*. We report, for the first time, parafrontal bones in *A. barbouri*, *A. expectatus*, *A. hechti*, *T. keyserlingii*, and *T. roborowskii*, and corroborate their presence in all species of *Aristelliger* and *Teratoscincus* except *A. reyesi* and *T. toksunicus* (not examined). No other gekkotans, either within or outside the Sphaerodactylidae, exhibited parafrontal bones. After examination of 111 osteological

prepared specimens (74 cleared-and-stained, 8 skeletonized, and 7 radiographed *Aristelliger*; 22 cleared-and-stained *Teratoscincus*), parafrontal bones were characterized based on bony plate shape, frontal-to-extra-brillar-fringe distance, and anterior-to-posterior distance. These measurements were often variable within conspecifics of the same size and asymmetrical within an individual. Bony plate counts of adult *Teratoscincus* were not correlated with parafrontal surface area ($r^2 = -0.02864$, $F = 0.6101$, $P = 0.4487$). Bony plate counts of adult *Aristelliger* are significantly correlated with parafrontal surface area ($r^2 = 0.2589$, $F = 16.02$, $P = 2.4 \times 10^{-4}$); however, the low r^2 value suggests this is negligible. For these reasons, parafrontal surface area was used as a measure of overall parafrontal size.

We found fibrous connective tissue sheets in the extra-brillar fringe of cleared-and-stained specimens of

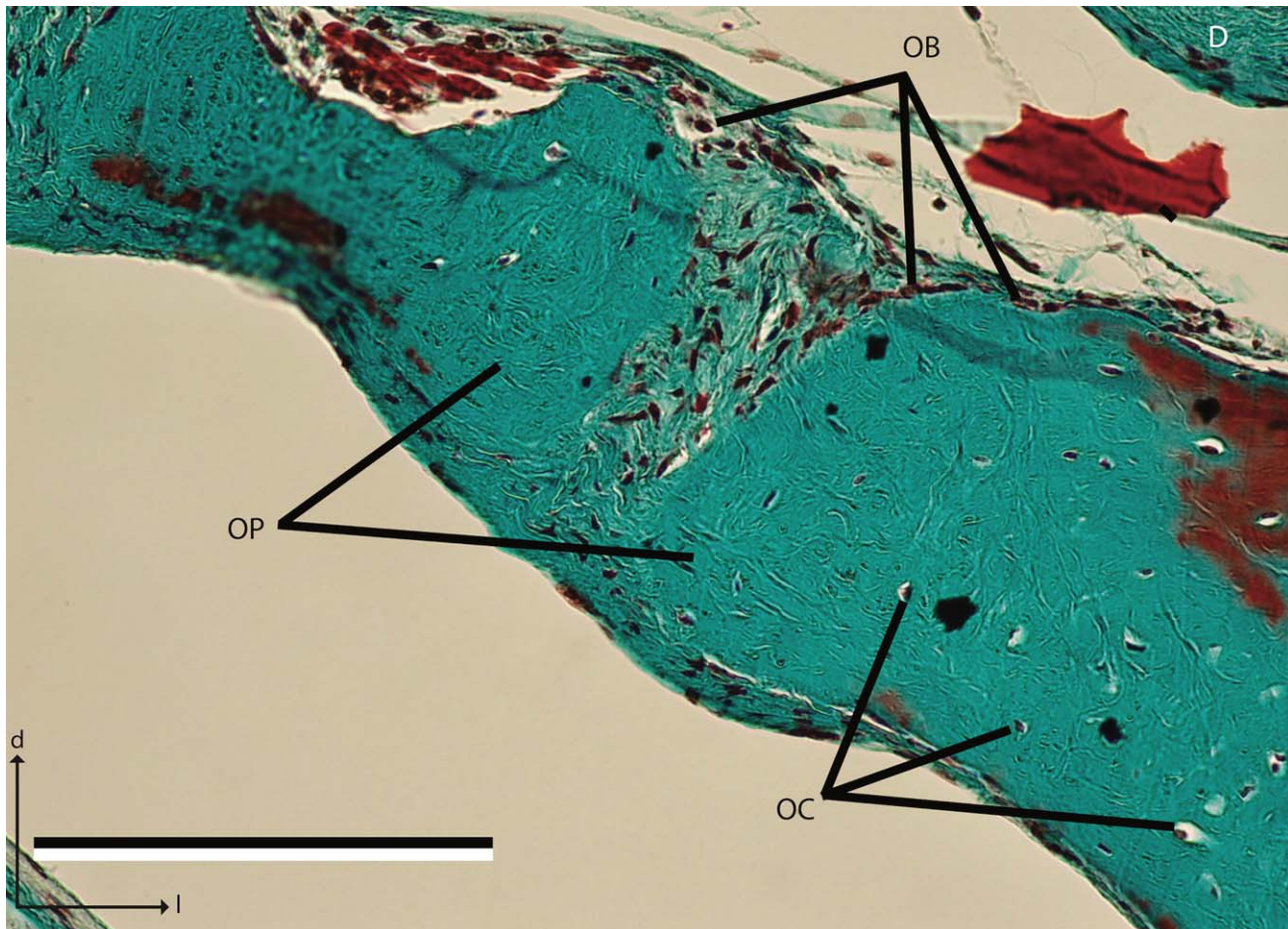


Fig. 4. Transverse section through the parafrontals of *Teratoscincus keyserlingii* (AMB 9210). D, dermis; OP, parafrontal bony plates; OC, osteocytes trapped within lacunae; OB, osteoblasts. Arrows indicate dorsal (d) and lateral (l) directions. Scale bar = 300 μm .

Aristelliger and *Teratoscincus*, as well as other members of this clade: *Sauromactylus fasciatus* (MVZ 162547), *Euleptes europaea* (NMNH 58963), *Quedenfeldtia trachyblepharus* (CM 55055A; Fig. 3), as noted by Daza et al. (2008). *Hemidactylus mabouia* (MCZ-A 27237; Gekkonidae), *Phelsuma madagascariensis* (CAS-SUR 13961; Gekkonidae), *Phelsuma sundbergi* (AMB 8435), *Rhacodactylus auriculatus* (CAS 165896; Diplodactylidae), and *Aleuroscalobotes felinus* (MVZ 111777; Eublepharidae) possess a connective tissue sheet in the supraorbital region that extends shallowly (~200 μm) into the extra-brillar fringe. Without cranial histological sections of these species, we cannot determine the composition of this connective tissue. The fibrous sheets of *Aristelliger*, *Euleptes*, *Quedenfeldtia*, and *S. fasciatus* occupy a smaller percentage of the extra-brillar fringe area than the ovoid sheet exhibited by *Teratoscincus*. Cleared-and-stained *Pristurus carteri* (MCZ 157119) and *Gonatodes ceciliae* (AMNH 108712) possess connective tissue extending laterally from the frontal, prefrontal, and postorbitofrontal bones into the extra-brillar fringe before eventually continuing with a ventrolateral inflection. Although superficially similar, this structure is less dense and less rigid than the fibrous sheets of *Aristelliger*, *Teratoscincus*, *Euleptes*, *Quedenfeldtia*, and *S.*

fasciatus and likely represent a loose connective tissue artifact resulting from removal of the eyes during the clearing and staining process. This is further supported by the absence of an obvious fibrous sheet in coronal cranial histosections of *G. ceciliae* (NMNH 349540, 349541, 349542). No other examined sphaerodactylid specimens possess obvious supraorbital structures. Several examined outgroup taxa possess firm connective tissue in the supraorbital region. Cleared-and-stained *Ptenopus garrulus* (CAS 8640, 8641, 8657; Gekkonidae) possesses large extra-brillar fringes containing connective tissue. Bellairs (1948) noted these remarkable extra-brillar fringes in his histological investigation of gecko spectacles. However, he did not illustrate the connective tissue or describe their histocomposition beyond being “thin” and “containing connective tissue and large blood-vessels.” In his illustrations of *Ptenopus*, the blank space adjacent to the frontal and between the dermis and the eye occupies the same plane and space as the fibrous sheet in *Aristelliger* and *Teratoscincus*. In cleared-and-stained specimens, this layer is grossly similar to the supraorbital fibrous sheet of *Aristelliger* and *Teratoscincus*, is rounded in shape, and has a greater relative surface area than the fibrous sheets of sphaerodactylids.

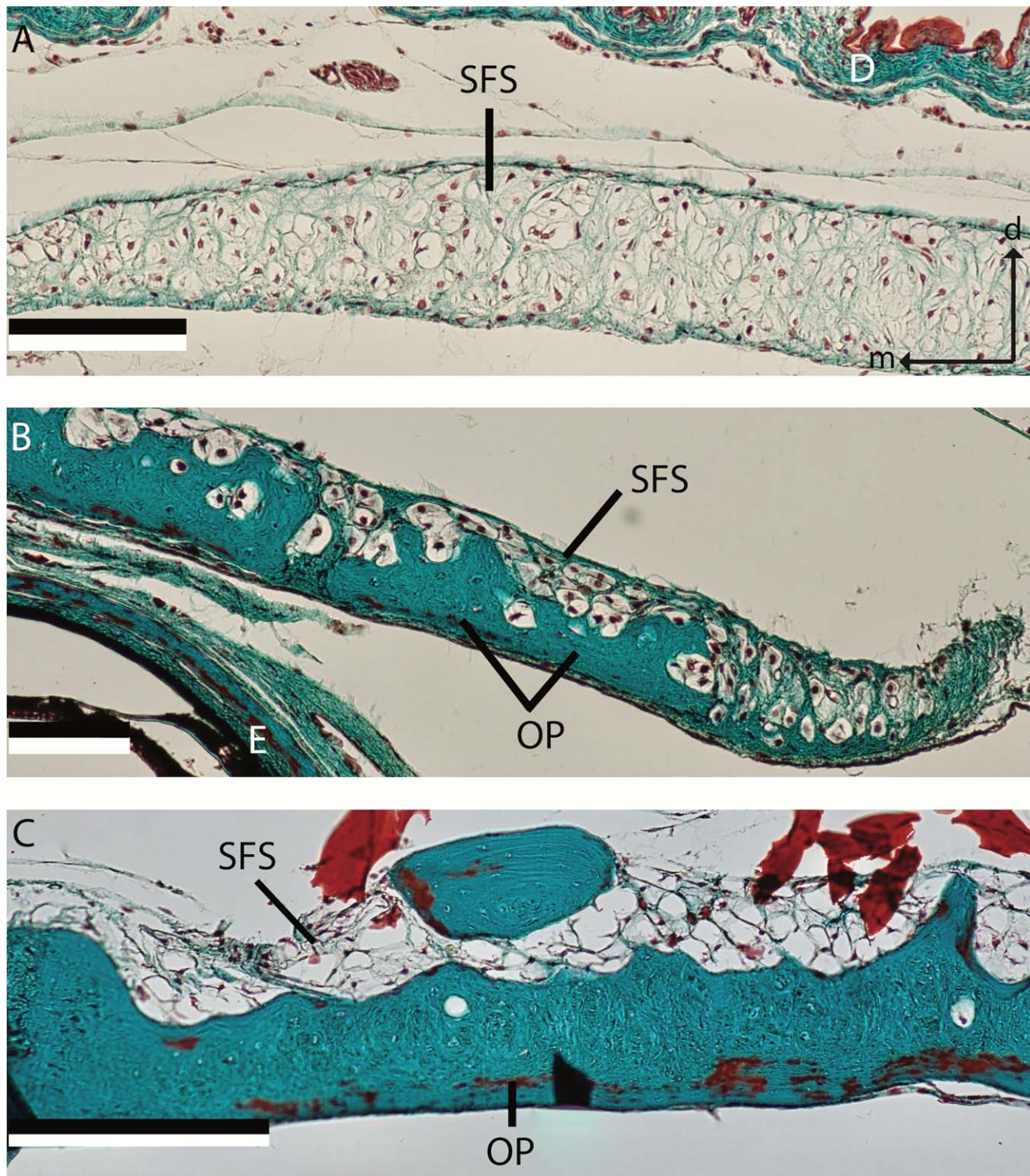


Fig. 5. Transverse sections of the supraorbital region of *Teratoscincus* through post-natal ontogeny. (A) *Teratoscincus przewalskii* (CAS 167423), 37.6 mm SVL; (B) *T. keyserlingii* (AMB 9211), 56.5 mm SVL; (C) *T. keyserlingii* (AMB 9210), 91.6 mm SVL. D, dermis; E, eye; OP, parafrontal bone; SFS, skeletogenic fibrous sheet. Arrows indicate dorsal (d) and medial (m) directions and apply to all panels. Scale bars = 300 μ m.

Histology of the supraorbital region of *Teratoscincus* and *Aristelliger* revealed that parafrontals develop directly from the supraorbital skeletogenic fibrous sheet.

In juvenile *Teratoscincus* the fibrous sheet is present prior to the formation of parafrontal bones, appears to contain numerous osteoblasts (Fig. 4), and extends into

the extra-brillar fringe (Fig. 5A). Later in ontogeny, a thin condensation of the tissue occurs in the ventral portion of the sheet, before eventually condensing in the dorsal direction, forming rugose, bony plates (Fig. 5B,C) similar to those originally described by Bauer and Russell (1989). At this ontogenetic stage, ossification occurs adjacent to the rim of the orbit, with portions of the unossified fibrous sheet still present in the most lateral portion of the parafrontals. In adults, the fibrous sheet matrix persists along the dorsal surface of the bony plates, with the latter including osteocytes within lacunae (Fig. 4). As seen in juvenile *Teratoscincus*, the fibrous sheet matrix is present prior to parafrontal ossification in juvenile *Aristelliger* (Fig. 6A). The presence of osteoblasts and osteocytes later in ontogeny suggests that the ossification of the parafrontal bones is not metaplastic (Haines and Mohuiddin, 1968; Sire et al., 2009; Fig. 6B). However, the matrix is denser than that of *Teratoscincus* and does not extend as far into the extra-brillar fringe. The developing bony plates replace the skeletogenic fibrous sheet, with the exception of a thin persistent layer adjacent to the dorsal surface of the smooth bony plates (Fig. 6B). Ossification of the fibrous sheet that lies between the orbital rim and the most medial parafrontal bony plates (Fig. 6B,C), and the resulting narrow interstices, accounts for the successful preservation of parafrontal bones in skeletonized specimens.

Parafrontal Development in *Aristelliger*

Bony plates were not present in embryos or hatchling specimens, suggesting that parafrontal bones ossify exclusively during postnatal development in *Aristelliger* (Figs. 7A,E,I and 8E,I). However, as reported in the histology results, the supraorbital skeletogenic fibrous sheet is present prior to parafrontal formation. A late-stage embryo of *Aristelliger barbouri* (AMB 9357) also exhibits this sheet, suggesting its prenatal presence in other *Aristelliger* species. Parafrontal development begins as numerous small, lozenge-shaped ossifications, forming adjacent to the orbital rim (Figs. (7 and 8), and 9). Later in ontogeny the bony condensations along the orbital rim coalesce, forming elongate plates, and smaller plates form more laterally to the orbital rim, within the extra-brillar fringe. In adults, parafrontal bones comprise numerous bony plates and collectively constitute a crescent-shape in the supraorbital region, with larger plates adjacent to and smaller plates further from the orbital rim.

In *Aristelliger barbouri* (Fig. 7A–D), the smallest species of *Aristelliger*, the onset of parafrontal development takes place later in ontogeny than most other examined species, between 24.4–36.7 mm SVL (49%–73% TBS). Approaching maximum body size (50 mm SVL; Schwartz and Henderson, 1991), parafrontal bones occupy a smaller portion of the supraorbital region than is the case for other species (Table 3), culminating in an elongate collection of thin bony plates, resembling the parafrontal bones of juveniles of larger-bodied *Aristelliger* species. In other small species of the subgenus *Aristelligera*, *A. cochranae* (Fig. 7E–H) and *A. expectatus* (Fig. 7I–L), parafrontal bones first appear between 26.9 and 41.6 mm SVL (38%–59% TBS) and 25.5 and 38.5 mm SVL (49%–74% TBS), respectively. Individuals

approaching the maximum body sizes for both species (63 and 52 mm SVL, respectively; Schwartz and Henderson, 1991), exhibit similar elongate collections of bony plates, but, these extend further laterally into the extra-brillar fringe and have considerably greater surface areas relative to skull length than do those of *A. barbouri* (Table 3). The onset of parafrontal ossification in larger species (subgenus *Aristelliger*) is variable. In *A. georgeensis* (Fig. 8A–D), the first visible bony plate develops at 33.6 mm SVL (29% TBS). In *A. praesignis* (Fig. 8I–L) and *A. hechti* (Fig. 9), parafrontal bones are already well-developed at 46.4 mm SVL (46% TBS) and 46.2 mm SVL (51% TBS), respectively. Initially parafrontal development between male and female *A. praesignis* follows similar ontogenetic trends of parafrontal surface area increase. However, as males eventually surpass females in SVL, the total parafrontal surface area of males becomes significantly larger (Wilcoxon signed-rank test, $P = 5.1 \times 10^{-10}$; R Core Team, 2014). In *A. lar* (Fig. 8E–H), the largest species of *Aristelliger*, the onset of parafrontal development does not occur until 43.4–64.2 mm SVL (32%–47% TBS). *Aristelliger lar* reaches the largest size before developing parafrontal bones (Figs. 8 and 10). Later in ontogeny of the larger *Aristelliger* species, bony plates adjacent to the margin of the orbit coalesce into 1–3 large, trapezoidal plates that border the lateral margin of the frontal. As smaller plates form further laterally, the collection of bony plates takes on an overall crescent shape that extends further laterally into the extra-brillar fringe than is the case for the smaller-bodied *Aristelliger* species. This results in a greater overall surface area when scaled to skull length (Table 3). In some cases, such as in adult *A. cochranae* (Fig. 7H), *A. georgeensis* (Fig. 8D), *A. lar* (Fig. 8H), and *A. praesignis* (Fig. 8L), parafrontal bones recess into the frontal, prefrontal, or postorbitofrontal.

Parafrontal Development in *Teratoscincus*

Similarly to parafrontal development in *Aristelliger*, parafrontal bones develop exclusively during postnatal ontogeny in *Teratoscincus*. The initial ossifications of *Teratoscincus* parafrontals express as numerous, small, lozenge-shaped bony plates which form adjacent to the orbital rim, thus resulting in larger plates that border the lateral margin of the frontal and smaller plates extending further laterally from the orbital rim (Figs. 11 and 12). In contrast to *Aristelliger*, the bony plates of *Teratoscincus* do not persist as elongate lozenge-, crescent-, or trapezoidal-shapes throughout ontogeny; but rather, they expand and coalesce with others and develop highly irregular outlines. Additionally, the bony plates of adult *Teratoscincus* are always more numerous than those of *Aristelliger* and occupy a greater area in the extra-brillar fringe (Tables 1 and 3; Fig. 13). The overall shape of the parafrontal bones is more variable than that of *Aristelliger*, culminating in an overall ovoid-shaped collection of plates in *T. scincus* (Fig. 11A–D), *T. keyserlingii* (Fig. 12D), and *T. roborskii* (Fig. 11I–L), a crescent-shaped collection in *T. microlepis* (Fig. 12C) and *T. bedriagai* (Fig. 11E–H), and an irregularly-shaped collection in *T. przewalskii* (Fig. 12A–B). At sizes approaching maximum body size (72 mm SVL; Anderson, 1999), the crescent-shaped collection of plates in the smallest species of *Teratoscincus*, *T. bedriagai*, occupy a smaller

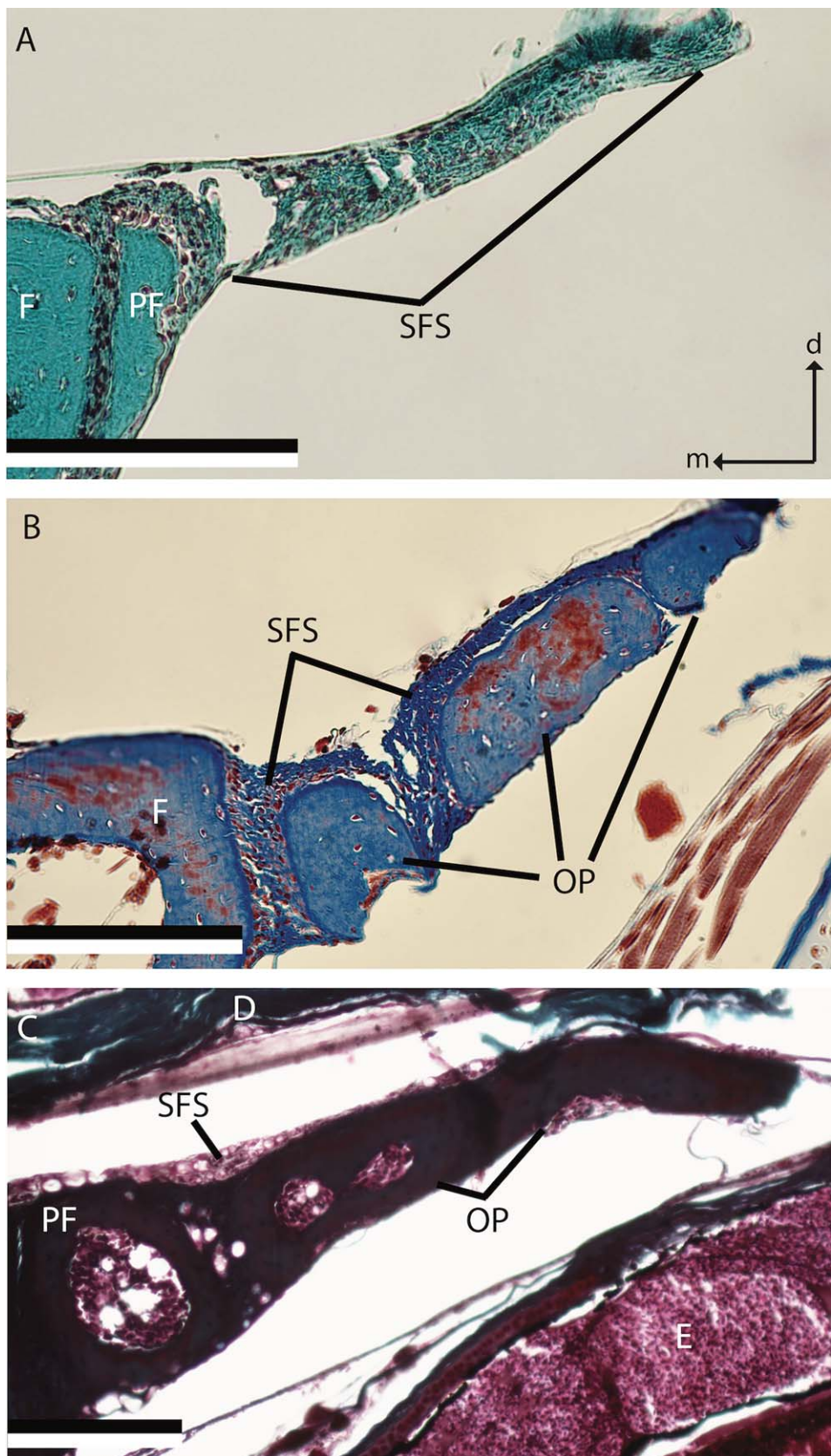


Fig. 6. Transverse sections of the supraorbital region of *Aristelliger praesignis* through post-natal ontogeny. (A) KU 228996, 29.9 mm SVL; (B) MCZ-A 36013, 45.5 mm SVL, Masson's Trichrome stain with aliphine blue instead of light green; and (C) estimated to be a subadult (slide from Bauer and Russell, 1989). D, dermis; E, eye; F, frontal; OP, parafrontal bones; PF, prefrontal; SFS, skeletogenic fibrous sheet. Arrows indicate dorsal (d) and medial (m) directions and apply to all panels. Scale bars = 300 μ m.

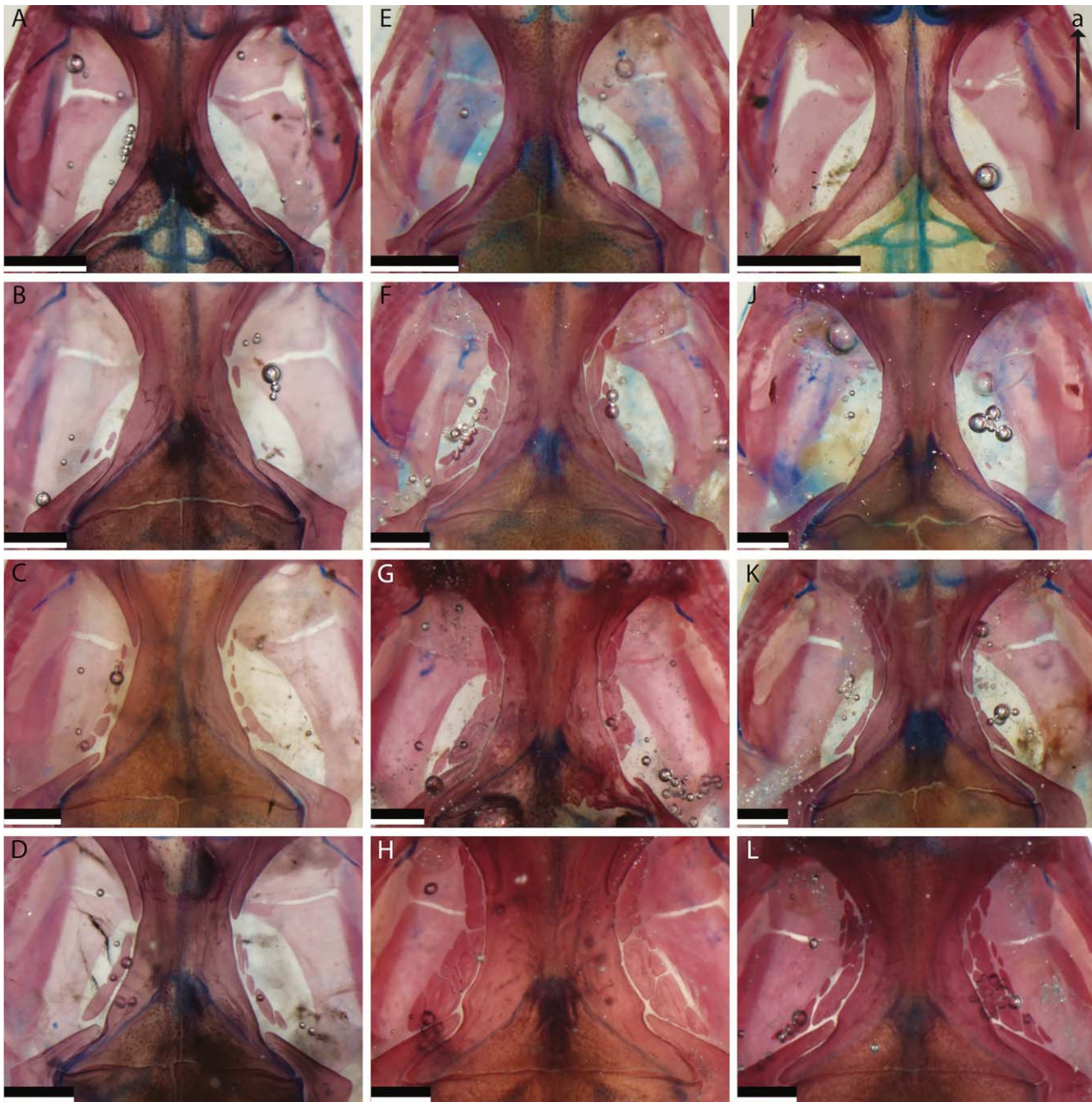


Fig. 7. Ontogenetic series of cleared-and-stained *Aristelliger* (Subgenus *Aristelligera*). Dorsal view of supraorbital region. (A) *A. barbouri*, AMB 9356, juvenile, 24.4 mm SVL; (B) *A. barbouri*, AMB 9354, subadult, 38.4 mm SVL; (C) *A. barbouri*, AMB 9352, adult, 41.6 mm SVL; (D) *A. barbouri*, AMB 9355, adult, 46.0 mm SVL; (E) *A. cochranae*, KU 228605, juvenile, 26.9 mm SVL; (F) *A. cochranae*, KU 228603, subadult, 41.6 mm SVL; (G) *A. cochranae*, KU 228597, subadult, 46.7 mm SVL; (H) *A. cochranae*, KU 228585, adult, 58.2 mm SVL; (I) *A. expectatus*, KU 228722, juvenile, 17.2 mm SVL; (J) *A. expectatus*, KU 228734, juvenile, 38.5 mm SVL; (K) *A. expectatus*, KU 228702, subadult, 41.6 mm SVL; and (L) *A. expectatus*, KU 228686, adult, 52.8 mm SVL. Arrow indicates the anterior (a) direction and applies to all panels. Scale bars = 1 mm.

portion of the supraorbital region when compared to the parafrontal bones of juveniles of larger-bodied *Teratoscincus* species.

The precise onset of parafrontal ossification in *Teratoscincus* is unknown. Of the *Teratoscincus* examined in this study, only two specimens, *T. przewalskii* (CAS

167421, 37.4 mm SVL, 40% TBS; Fig. 12A) and *T. scincus* (CAS 199550, 42.0 mm SVL, 36% TBS; Fig. 11A), did not exhibit bony plates early in ontogeny. Within these ontogenetic series, the next largest specimens are over 20 mm SVL longer and have well-developed parafrontal bones, indicating that parafrontal bones begin

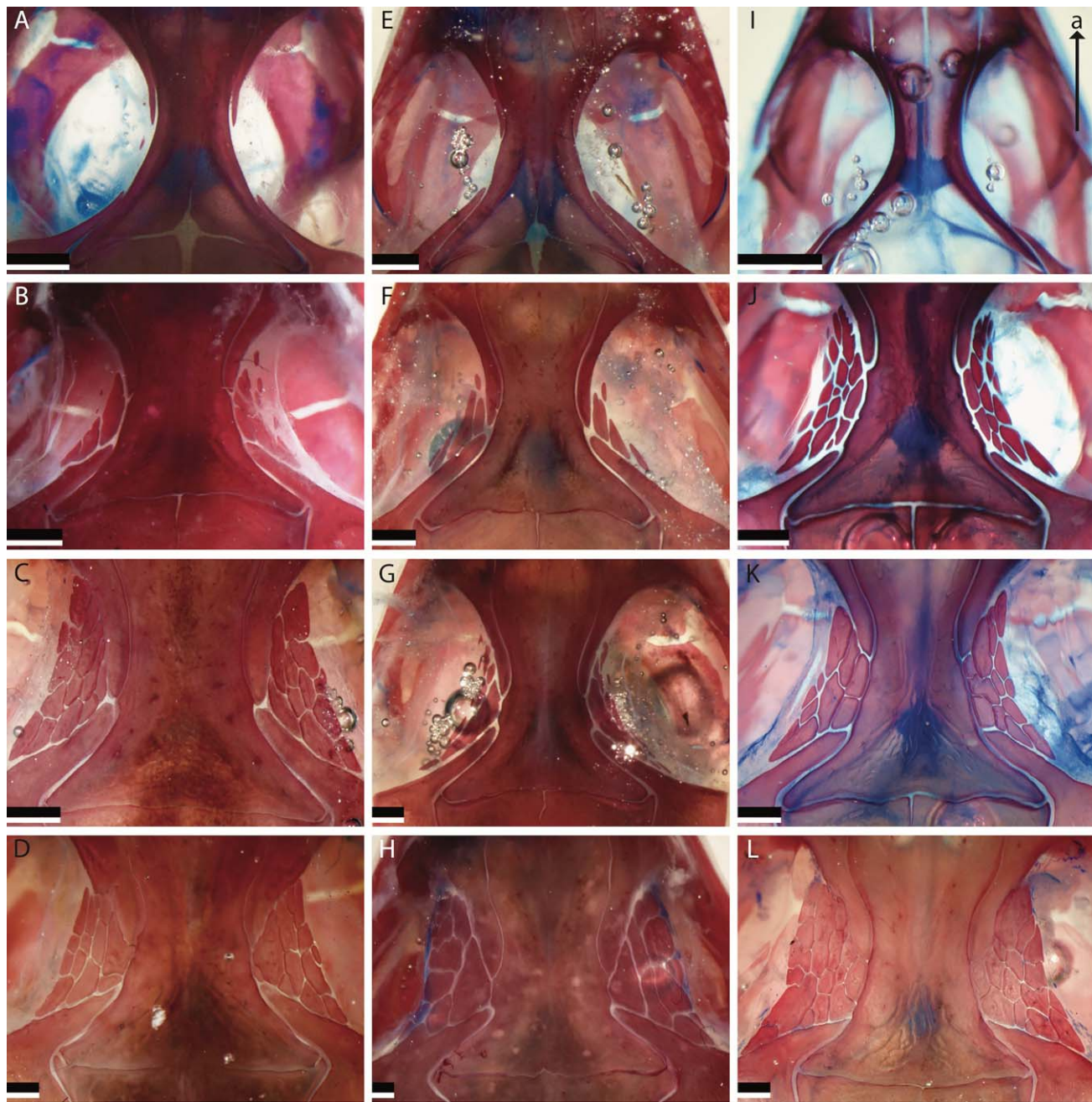


Fig. 8. Ontogenetic series of cleared-and-stained *Aristelliger* (Subgenus *Aristelliger*). Dorsal view of supraorbital region. (A) *A. georgeensis*, UCM 16183, juvenile, 33.6 mm SVL; (B) *A. georgeensis*, UCM 16184, subadult, 52.7 mm SVL; (C) *A. georgeensis*, KU 070030, adult, 78.9 mm SVL; (D) *A. georgeensis*, KU 070027, adult, 95.6 mm SVL; (E) *A. lar*, KU 228760, juvenile, 43.4 mm SVL; (F) *A. lar*, KU 228795, juvenile, 64.2 mm SVL; (G) *A. lar*, KU 228792, subadult, 70.9 mm SVL; (H) *A. lar*, KU 228785, adult, 129.9 mm SVL; (I) *A. praesignis*, MCZ R-194571, juvenile, 23.0 mm SVL; (J) *A. praesignis*, MCZ R-194588, subadult, 60.8 mm SVL; (K) *A. praesignis*, MCZ R-194575, adult, 74.9 mm SVL; and (L) *A. praesignis*, MCZ R-194594, adult, 98 mm SVL. Arrow indicates the anterior (a) direction and applies to all panels. Scale bars = 1 mm.

ossification at somewhere between 37.4 and 82.5 mm SVL (40%–69% TBS) and 42.0–64.0 mm SVL (36%–55% TBS) in *T. przewalskii* and *T. scincus*, respectively. The parafrontal bones of *T. roborowskii* (Fig. 11I–L) begin ossifying shortly before 44.2 mm SVL (51% TBS). The parafrontal bones of *T. bedriagai* (Fig. 11E–H), *T. microlepis*

(Fig. 12C), and *T. keyserlingii* (Fig. 12D) are well-developed by 56.2 mm SVL (75% TBS), 43.3 mm SVL (56% TBS), and 84.6 mm SVL (73% TBS), respectively. The exclusively postnatal parafrontal development exhibited by *T. przewalskii* and *T. scincus* is consistent with the parafrontal development exhibited by *Aristelliger*.

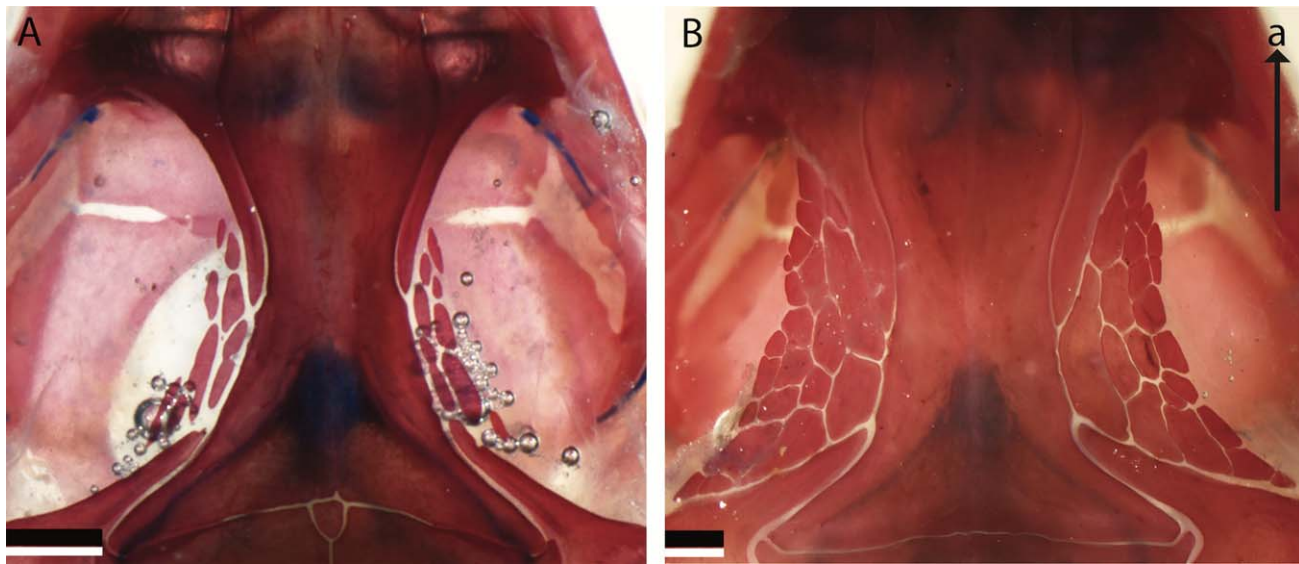


Fig. 9. Cleared-and-stained *Aristelliger hechti*. Dorsal view of supraorbital region. (A) KU 228758, subadult, 46.4 mm SVL and (B) KU 228757, adult, 86.4 mm SVL. Arrow indicates the anterior (a) direction and applies to all panels. Scale bars = 1 mm.

TABLE 3. The largest parafrontal surface areas for each *Aristelliger* and *Teratoscincus* species examined in this study scaled to skull length

ID	Species	SL (mm)	Bony plates	Surface area (mm ²)	Scaled surface area (mm ²)
AMNH 45811	<i>A. barbouri</i>	14.7	7	0.69	0.05
KU 228686	<i>A. expectatus</i>	14.3	27	1.83	0.13
USNM 305438	<i>A. cochranae</i>	20.2	15	9.01	0.45
KU 070027	<i>A. georgeensis</i>	25.9	26	9.87	0.36
MCZ R194592	<i>A. praesignis</i>	24.9	68	19.33	0.78
KU 228757	<i>A. hechti</i>	23.1	43	21.33	0.92
KU 228785	<i>A. lar</i>	35.5	26	36.35	1.02
CAS 228581	<i>T. bedriagai</i>	17.8	70	13.53	0.76
CAS 1677391	<i>T. przewalskii</i>	22.6	30	24.40	1.08
MVZ 243568	<i>T. microlepis</i>	19.1	42	20.83	1.09
CAS 168055	<i>T. roborowskii</i>	24.7	76	28.60	1.16
CAS 228807	<i>T. keyserlingii</i>	22.5	54	35.34	1.57
CAS 101437	<i>T. scincus</i>	25.8	73	51.64	2.00

Corresponding skull lengths (SL), total bony plate counts, and total surface areas are included.

DISCUSSION

Homology and Evolution of Parafrontal Bones

At its simplest, homology can be defined as similarity due to common ancestry (reviewed in Wake et al., 2011). Often this similarity refers to a morphological character and can be identified by a combination of conditions: close phylogenetic relatedness of the taxa in which the character is present; conservation of structure and position of the character; and similar developmental origins ("uniqueness," "conservation," and "individuality," *sensu* Wagner, 1989). The condensation of parafrontal bones occurs within the supraorbital skeletogenic fibrous sheet, in the absence of a cartilaginous precursor. Additionally, parafrontal bones of *Aristelliger* and *Teratoscincus* exhibit a similar postnatal onset of ossification and overall pattern of ossification. The presence of firm, supraorbital fibrous sheets in *Quedenfeldtia*, *Sauromaculatus fasciatus*, and *Euleptes* supports the interpretation

of this feature as a putative synapomorphy of this clade of sphaerodactylids. However further histological examination of the frontal region of *Pristurus* and *Gonatodes ceciliae* is needed to corroborate the absence of this fibrous sheet outside the clade containing *Aristelliger* and *Teratoscincus*. The close phylogenetic relationship between *Aristelliger* and *Teratoscincus*, the similar anatomy and position of their parafrontal bones, and the developmental data from this study, suggest that parafrontal bones result from parallel evolution, developing from a homologous skeletogenic fibrous sheet. Geckos exhibit similar parallel evolution of adhesive toepads (Russell, 1979; Gamble et al., 2012). The spinulate Oberhäutchen layer of the gekkotan subdigital epidermis is an ancestral trait (Maderson, 1970; Stewart and Daniel, 1972; Russell, 1979; Peattie, 2008), which serves as a necessary precursor for further elaborations of the condition, resulting in multiple, parallel but not wholly independent, derivations of toepads. We propose that

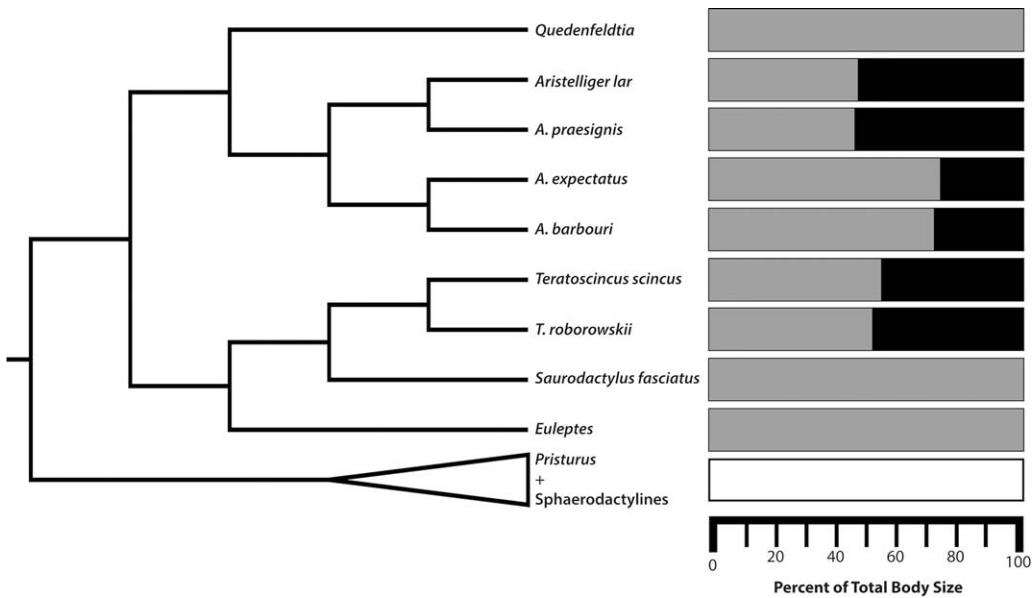


Fig. 10. Supraorbital development corresponding to the percent of total body size for each respective sphaerodactylid lineage. White indicates the absence of parafrontals and a supraorbital mesenchymal sheet, gray indicates the presence of a supraorbital fibrous sheet without parafrontals, and black indicates the presence of both parafrontals and a supraorbital fibrous sheet. Phylogeny adapted from Gamble et al. (2015b).

parafrontal bones are parallel elaborations within the homologous supraorbital fibrous sheet.

Considering the lack of a cartilaginous precursor and the tendency for parafrontals to coalesce with the prefrontals, frontals, and postorbitofrontals, we consider parafrontals to be lateral extensions of the dermal bone roofing series. A potential genetic underpinning of parafrontal expression can be attributed to the *Sp7/Osterix* zinc finger transcription factor, which is required for osteoblast differentiation in vertebrates (Nakashima et al., 2002). In zebrafish (*Danio rerio*), *sp7/osterix* mutants exhibit delayed and abnormal postnatal craniofacial ossification (Kague et al., 2016). Such abnormalities include atypical distribution of bony fragments in and around the frontals and parietals, as well as a failure of sutures to fuse. We hypothesize that *Sp7/Osterix* expression is disrupted in the extra-brillar fringe of *Aristelliger* and *Teratoscincus* area and results in the irregular postnatal ossifications that comprise parafrontal bones. The functional significance of parafrontal bones, if any, remains enigmatic. If there is no adaptive significance to possessing parafrontal bones, a possible non-functional explanation could be directional selection upon a pleiotropic gene (Atchley and Hall, 1991). A possible function of parafrontal bones could be to serve as a connection point related to the kinetic articulations that are typical of gecko skulls. The supraorbital bone of *Loxocemus* (Loxocemidae) and pythonid snakes occupies a similar position to parafrontal bones. Although this bone is not homologous to parafrontal bones, it, along with the rest of the circumorbital bones, provides an important, kinetic connection between the upper jaw and braincase (Cundall and Irish, 2008). Gekkotans, much like snakes, and unlike other non-ophidian squamates, possess highly kinetic skulls with reduced temporal arcades (Evans, 2008). Sphaerodactyls, relative to other

geckos, possess highly reduced skulls (Daza et al., 2008; Fig. 2C). Therefore, additional connection between the rostral region and braincase, via a dorso-orbital connection (i.e., prefrontal, parafrontal bones, and postorbitofrontal), may facilitate similar cranial kinesis in the larger skulls of *Aristelliger* and *Teratoscincus*. However, the closest joint associated with kinesis is a mesokinetic joint between the frontal and the parietals (Herrel et al., 1999), and no ligaments, tendons, or muscles connecting the supraorbital region to the mesokinetic joint have been identified. A clear correlate of parafrontal bones is a reduction of the dorsal bulging of the eyes, as exhibited in miniaturized sphaerodactyls (Daza et al., 2008). The presence of two foveae within the eyes of sphaerodactyls suggests that dorsal bulging is an adaptation for binocular vision (Röll, 2001). It is likely that binocular visual capability is limited in *Aristelliger* and *Teratoscincus*, and that these may exhibit a different field of vision. This reduction in dorsal bulging may have facilitated the condensation of the skeletogenic fibrous sheet.

Further functional capabilities of parafrontal bones can be inferred from the natural history of *Aristelliger* and *Teratoscincus*. The gekkonid *Ptenopus*, which possesses an extended extra-brillar fringe and dense supraorbital connective tissue, is a burrowing gecko (Haacke, 1975). *Teratoscincus* has also been noted to burrow (Szczerbak and Golubev, 1996; Anderson, 1999), and *Aristelliger* is known to inhabit crevices of trees (Henderson and Powell, 2009). Additional protection over the orbits of these ablepharous lizards may prevent debris, associated with burrow or crevice excavation or disturbance, from damaging their eyes. The need for supraorbital protection may also be explained by interactions occurring during intraspecific aggression. Vickaryous et al. (2015) hypothesized that the robust osteoderms in the supraorbital region of

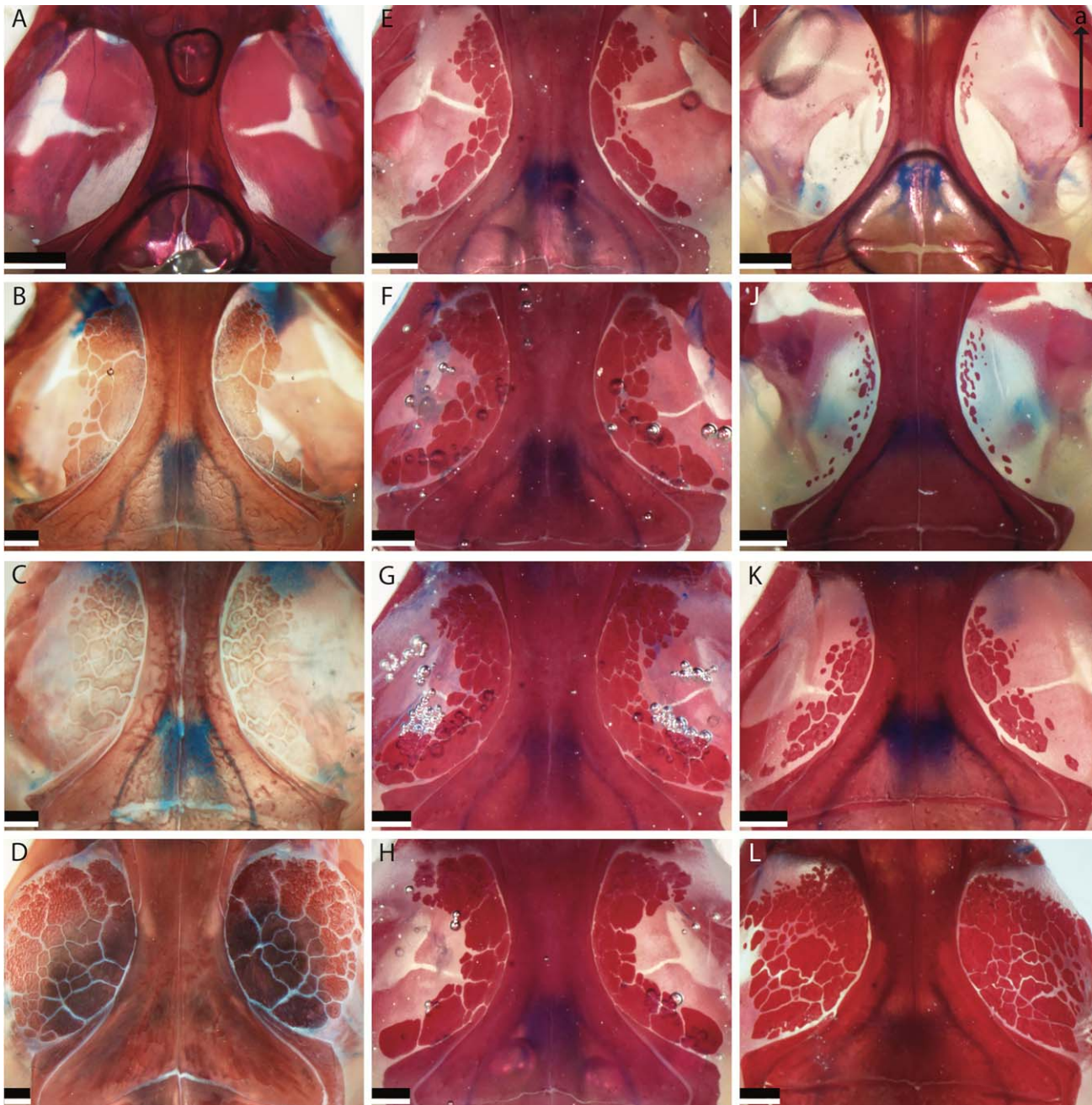


Fig. 11. Ontogenetic series of cleared-and-stained *Teratoscincus*. Dorsal view of supraorbital region. (A) *T. scincus*, CAS 199550, juvenile, 42.0 mm SVL; (B) *T. scincus*, AMB 1237, subadult, 64.0 mm SVL; (C) *T. scincus*, AMB 1238, subadult, 65.5 mm SVL; (D) *T. scincus*, CAS 101437, adult, 97.0 mm SVL; (E) *T. bedriagai*, MVZ 236999, juvenile, 56.2 mm SVL; (F) *T. bedriagai*, MVZ 237000, subadult, 60.0 mm SVL; (G) *T. bedriagai*, MVZ 237001, adult, 62.3 mm SVL; (H) *T. bedriagai*, MVZ 237002, adult, 63.4 mm SVL; (I) *T. roborowskii*, MVZ 208967, juvenile, 44.2 mm SVL; (J) *T. roborowskii*, CAS 168088, juvenile, 48.5 mm SVL; (K) *T. roborowskii*, MVZ 208966, subadult, 60.6 mm SVL; and (L) *T. roborowskii*, MVZ 208965, adult, 69.3 mm SVL. Arrow indicates the anterior (a) direction and applies to all panels. Scale bars = 1 mm.

Tarentola (Fig. 14) are used for protection from territorial conspecifics. Similarly, *Teratoscincus* has been noted to be aggressive and territorial, particularly gravid females (Szczerbak and Golubev, 1996). Across sphaerodactylids, females are generally larger in size than males (Fitch, 1981; Cox and Kahrl, 2014),

although our field-collected series of *Aristelliger praesignis* exhibits significant male-biased sexual size dimorphism (77.5% average Female–Male Ratio *sensu* Fitch, 1981; Wilcoxon signed-rank test, $P = 0.001$; R Core Team, 2014). Extremely large *A. praesignis* males often show signs of intraspecific attack: scarred bite-

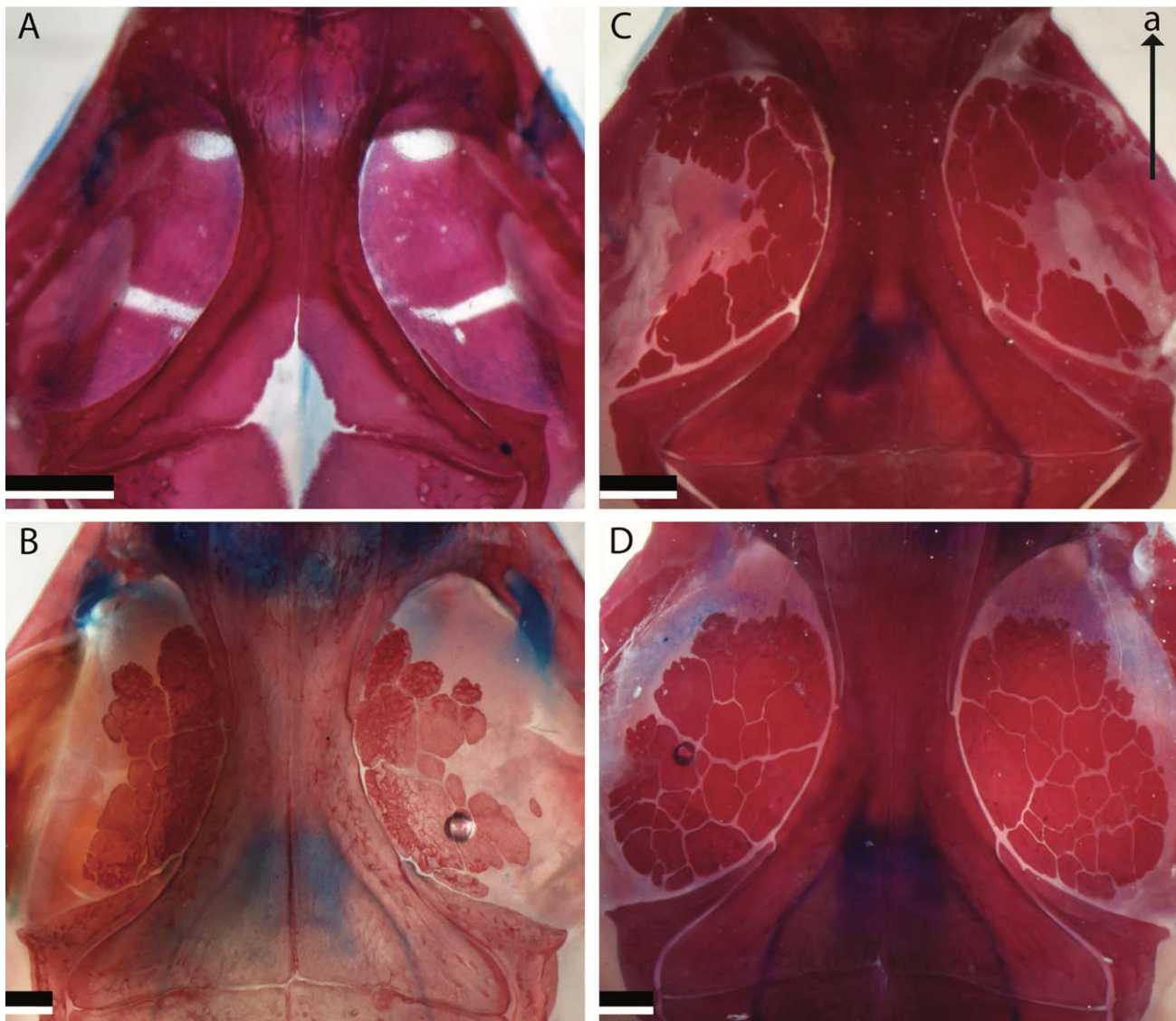


Fig. 12. Cleared-and-stained *Teratoscincus*. Dorsal view of supraorbital region. (A) *T. przewalskii*, CAS 167421, juvenile, 37.4 mm SVL; (B) *T. przewalskii*, CAS 167391, adult, 85.5 mm SVL; (C) *T. microlepis*, MVZ 243568, subadult, 43.3 mm SVL; and (D) *T. keyserlingii*, CAS 228807, adult, 84.6 mm SVL. Arrow indicates the anterior (a) direction and applies to all panels. Scale bars = 1 mm.

marks on the head and torso, missing digits, and occasionally a missing full manus. This suggests that larger *Aristelliger* species are likely subject to intraspecific aggression. Supraorbital protection, via parafrontal bones, may protect the eyes from conspecific attack. Future analysis of sexual shape dimorphism in parafrontal bones may elucidate their possible ecological function.

Parafrontal Bones, Sphaerodactylid Body Size, and Ontogeny

The ranges of sphaerodactylid body size and the current phylogenetic hypothesis of relationships suggest that ancestral sphaerodactylids were small-bodied (Fig. 1), though miniaturization is likely not the plesiomorphic condition. Overlap in body size, between other

sphaerodactylids and *Aristelliger* and *Teratoscincus* large enough to possess parafrontal bones, suggests that there is not a strict threshold body size below which parafrontal bones do not develop. The smallest skull length at which parafrontal bones were observed was 10.0 mm in *Aristelliger barbouri*. The absence of parafrontal bones and skull lengths above 10.0 mm in *Gonatodes*, *Sphaerodactylus*, and *Pristurus* would suggest clade specificity for a threshold parafrontal development body size. However, the absence of parafrontal bones and skull lengths above 10.0 mm in *Euleptes* and *Quedenfeldtia*, members of the clade to which *Aristelliger* and *Teratoscincus* belong, does not support this hypothesis. Heterochronic processes may partially explain the presence and development of parafrontal bones. The late postnatal appearance of parafrontal bones in *Aristelliger* and *Teratoscincus* suggests parafrontals are the

result of peramorphic processes (Alberch et al., 1979; McNamara, 1986). Peramorphosis, via hypermorphosis, is supported in *Aristelliger* due to their overall large size, osteological novelty (i.e., parafrontal bones and hemipenial bones; Kluge, 1982), and peramorphic character states (e.g., postorbitofrontals with a dorsal shelf supporting the parietals, fused parietals, tall coronoid process; Daza et al., 2015). However, peramorphosis would not likely explain the presence of parafrontal bones in *Teratoscincus*, which is considered to possess paedomorphic character states. The overall large body size, reduction in cranial fusion (e.g., paired frontals),

and large orbits suggest *Teratoscincus* is neotenic (Stephenson and Stephenson, 1956; Alberch et al., 1979; Bauer, 1986; McNamara, 1986). However, modularity likely exists in the developmental trajectories of the gekkotan circumorbital bones and evidence exists for the influence of adult size on embryo cell number (Alberch, 1985). Such developmental constraints could force the presence of parafrontal bones in adults of *Aristelliger* and *Teratoscincus*, while precluding their presence in other sphaerodactylids. Parafrontal bones develop between 29% and 75% TBS in most *Aristelliger* and *Teratoscincus* we examined. Although further ontogenetic sampling of *A. hechti*, *A. reyesi*, *T. bedriagai*, *T. microlepis*, and *T. keyserlingii* is needed to corroborate the exclusive postnatal development of parafrontal bones in all taxa and to identify a more precise ontogenetic period in which parafrontal bones develop in these species. Either peramorphosis and paedomorphosis can explain the differences in parafrontal surface area and overall morphology within the genus *Aristelliger*. The earlier onset (i.e., predisplacement) of parafrontal development in large species of *Aristelliger* (29%–47% TBS; *A. georgeensis*, *A. lar*, *A. praesignis*; Fig. 10) compared to smaller species of *Aristelliger* (59%–74% TBS; *A. barbouri*, *A. cochranae*, *A. expectatus*; Fig. 10) and *Teratoscincus* (51%–65% TBS; *T. przewalskii*, *T. roborskii*, *T. scincus*; Fig. 10) could suggest that larger *Aristelliger* are peramorphic (Alberch et al., 1979). Alternatively, if large species represent the ancestral ontogenetic trajectory for the genus, the extremely late onset of parafrontal development in small species of *Aristelliger* could be interpreted as postdisplacement, implying that the small forms are paedomorphic (Alberch et al., 1979). The current hypothesis of *Aristelliger* relationships

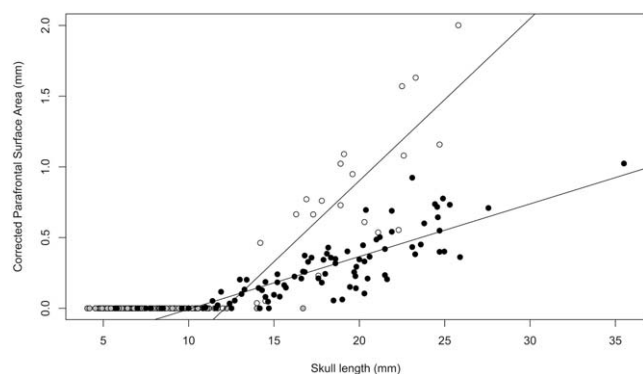


Fig. 13. Parafrontal surface area, scaled to skull length, for all sphaerodactylids examined in this study. Black circles, white circles, and gray circles correspond to an *Aristelliger*, *Teratoscincus*, and other sphaerodactylid specimens, respectively. The scaled parafrontal surface areas for *Aristelliger* and *Teratoscincus* differ significantly (ANCOVA, $P = 3.94 \times 10^{-9}$).

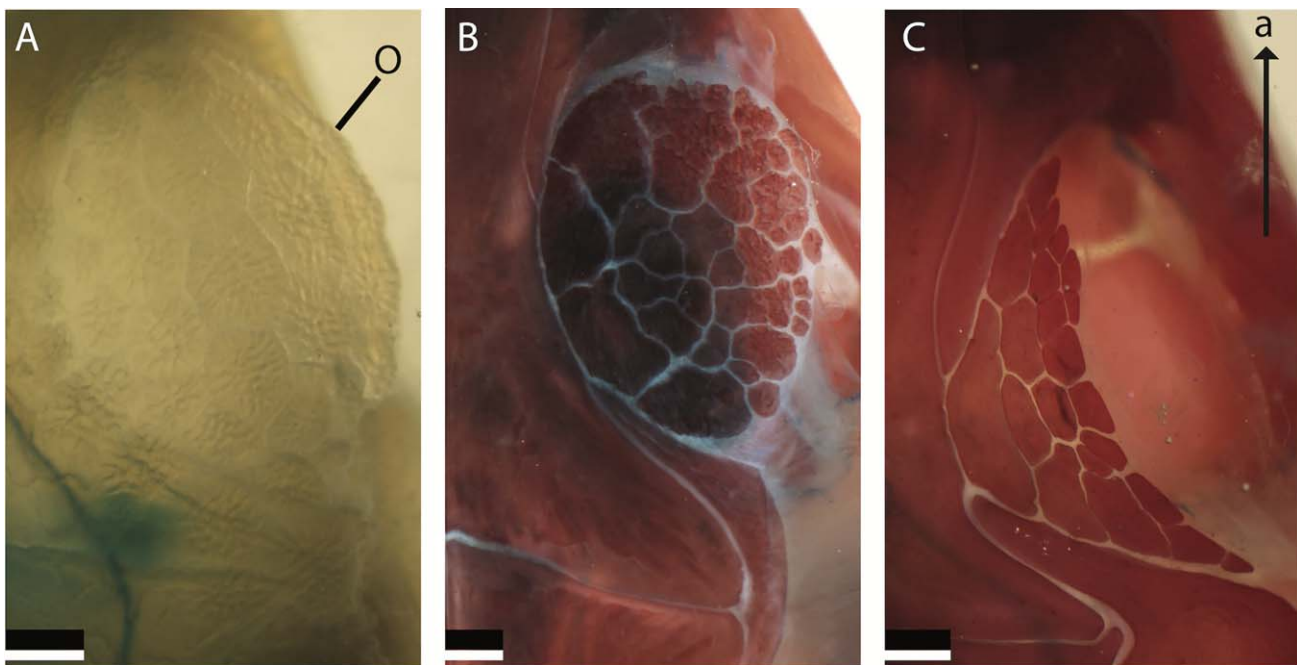


Fig. 14. Dorsal view of the frontal region of cleared-and-stained. (A) *Tarentola chazaliae* (AMB 1455), (B) *Teratoscincus scincus* (CAS 101437), (C) *Aristelliger hechti* (KU 228757). Arrow indicates the anterior (a) direction and applies to all panels. Scale bar = 1 mm. O, supraorbital osteoderms.

suggest that large species (subgenus *Aristelliger*) and small species (subgenus *Aristelligella*) are sister clades (Cloud, 2013) and that the sister lineage to *Aristelliger* as a whole is a small-bodied genus, *Quedenfeldtia* (Gamble et al., 2015b). Given this, we hypothesize that the condition exhibited by small-bodied *Aristelliger* is likely ancestral to the genus, implying that larger *Aristelliger* are peramorphic.

CONCLUSIONS

The parafrontals of *Aristelliger* and *Teratoscincus* have homologous developmental origins. Furthermore, the identification of the supraorbital skeletogenic fibrous sheets in the clade to which these taxa belong suggests this character may be useful for future phylogenetic analyses. This precursor to parafrontal bones is only found in the sphaerodactylid clade containing *Aristelliger*, *Teratoscincus*, *Quedenfeldtia*, *Euleptes*, and *Sauromadtylus fasciatus*, regardless of the maximum body size of any of the included taxa (Fig. 10). Within this clade, there is not a definitive threshold body size below which parafrontal bones do not develop; however, the onset of parafrontal development occurs between 38 and 64 mm SVL in *Aristelliger* and *Teratoscincus*. These lineages, including the relatively small-bodied *A. barbouri*, reach maximum sizes exceeding those of *Quedenfeldtia*, *Euleptes*, and *S. fasciatus* (Fig. 10), suggesting that large body size is associated with the development of parafrontal bones within this clade. Within these large-bodied lineages, the onset of parafrontal development differs between individual species (Fig. 10). The possible heterochronic processes occurring, specifically in *Aristelliger*, indicate that ontogenetic stage is an important factor in formation of parafrontal bones. Therefore, the presence of parafrontal bones cannot be explained by phylogeny, body size evolution, or shifts in ontogenetic trajectory alone; but rather all three of these processes likely contribute to the evolution and development of these novel structures.

ACKNOWLEDGMENTS

We gratefully acknowledge funding from the Villanova University Department of Biology and School of Graduate Arts and Sciences, the Gerald E. Lemole Chair Fund, the Gans Charitable Collection, and the Society for the Study of Amphibians and Reptiles. We thank all institutional collections and associated collection managers who loaned specimens for this study. We also thank Tim Tytle Lizards for providing captive-raised *Teratoscincus*. Field collection of many *Aristelliger* specimens would not have been possible without the assistance from the Bahamas National Trust, Jamaican National Environment & Planning Agency, Randolph Burrows, Dr. Byron Wilson, and Dr. Michael Rowe. We also thank Daniel Paluh for providing µCT images for this study. Additionally, we thank Kenneth Tighe and Addison Wynn for radiograph images. An earlier version of this manuscript benefitted immensely from the helpful comments and critiques of three anonymous reviewers. This study represents the result of thesis research in partial fulfillment of a Master of Science in Biology degree from Villanova University awarded to AHG.

LITERATURE CITED

- Abzhanov A, Rodda SJ, McMahon AP, Tabin CJ. 2007. Regulation of skeletogenic differentiation in cranial dermal bone. *Development* 134:3133–3144.
- Alberch P, Gould SJ, Oster GF, Wake DB. 1979. Size and shape in ontogeny and phylogeny. *Paleobiology* 5:296–317.
- Alberch P. 1985. Developmental constraints: Why St. Bernards often have an extra digit and poodles never do. *Am Nat* 126:430–433.
- Anderson SC. 1999. *The Lizards of Iran*. Ithaca: Society for the Study of Amphibians and Reptiles.
- Atchley WR, Hall BK. 1991. A model for development and evolution of complex morphological structures. *Biol Rev* 66:101–157.
- Avila-Pires TCS. 1995. *Lizards of Brazilian Amazonia* (Reptilia: Squamata). Zool Verhandel 299:1–706.
- Barrio-Amorós CL, Brewer-Carías C. 2008. Herpetological results of the 2002 expedition to Sararínamá, a tepui in Venezuelan Guyana, with the description of five new species. *Zootaxa* 1942:1–68.
- Batista A, Ponce M, Vesely M, Mebert K, Hertz A, Köhler G, Carrizo A, Lotzkat S. 2015. Revision of the genus *Lepidoblepharis* (Reptilia: Squamata: Sphaerodactylidae) in Central America, with the description of three new species. *Zootaxa* 3994:187–221.
- Bauer AM. 1986. Systematics, biogeography and evolutionary morphology of the Carphodactylini (Reptilia: Gekkonidae). Doctoral Dissertation, University of California, Berkeley.
- Bauer AM, Russell AP. 1989. Supraorbital ossifications in geckos (Reptilia: Gekkonidae). *Can J Zool* 67:678–684.
- Bellairs AD'A. 2009. The eyelids and spectacle in geckos. *Proc Zool Soc Lond* 118:420–425.
- Blanford WT. 2009. Notes on the lizards collected in Socotra by Prof. I. Bayley Balfour. *Proc Zool Soc Lond* 49:464–469.
- Calderón-Espinosa ML, Medina-Rangel GF. 2016. A new *Lepidoblepharis* lizard (Squamata: Sphaerodactylidae) from the Colombian Guyana shield. *Zootaxa* 4067:215–232.
- Cartier O. 1872. Studien über den feineren Bau der Epidermis bei den Geckotiden. *Verh Wurzbh Physiol-Med Ges NF* 3:Bd.
- Cloud TL. 2013. Cryptic diversity, evolution, and biogeography of Caribbean croaking geckos (Genus: *Aristelliger*). Master's Thesis, Pennsylvania State University.
- Conrad JL. 2004. Is the “stem-gecko” body plan really plesiomorphic for Squamata. *J Morphol* 260:284.
- Conroy CJ, Papenfuss T, Parker J, Hahn NE. 2009. Use of tricaine methanesulfonate (MS222) for euthanasia of reptiles. *J Am Assoc Lab Anim Sci* 48:28–32.
- Cox RM, Kahrl AF. 2014. Sexual selection and sexual dimorphism. In: Rheubert JL, Siegel DS, Trauth SE, editors. *Reproductive Biology and Phylogeny of Lizards and Tuatara*. Boca Raton: CRC Press. p 78–108.
- Cundall D, Irish F. 2008. The snake skull. In: Gans C, Gaunt AS, Alder K, editors. *Biology of the Reptilia: Morphology H: The Skull of Lepidosauria* (Vol. 20). Ithaca: Society for the Study of Amphibians & Reptiles. p 349–692.
- Daza JD, Abdala V, Thomas R, Bauer AM. 2008. Skull anatomy of the miniaturized gecko *Sphaerodactylus roosevelti* (Squamata: Gekkota). *J Morphol* 269:1340–1364.
- Daza JD, Bauer AM. 2010. The circumorbital bones of the Gekkota (Reptilia: Squamata). *Anat Rec* 293:402–413.
- Daza JD, Bauer AM. 2012. A new amber-embedded sphaerodactyl gecko from Hispaniola, with comments on morphological synapomorphies of the Sphaerodactylidae. *Breviora* 529:1–28.
- Daza JD, Mapps AA, Lewis PJ, Thies ML, Bauer AM. 2015. Peramorphic traits in the tokay gecko skull. *J Morphol* 276:915–928.
- Díaz LM, Hedges SB. 2009. First record of the genus *Aristelliger* (Squamata: Sphaerodactylidae) in Cuba, with description of a new species. *Zootaxa* 2028:31–40.
- Evans SE. 2008. The skull of lizards and tuatara. In: Gans C, Gaunt AS, Alder K, editors. *Biology of the Reptilia: Morphology H: The Skull of Lepidosauria* (Vol. 20). Ithaca: Society for the Study of Amphibians & Reptiles. p 1–347.
- Fitch HS. 1981. Sexual size differences in reptiles. *Misc Publ Univ Kans Mus Nat Hist* 70:1–72.

- Fong A, Díaz LM. 2004. Two new species of *Sphaerodactylus* (Sauria: Gekkonidae) from the southeastern coast of Cuba. *Solenodon* 4:73–84.
- Gamble T, Bauer AM, Greenbaum E, Jackman TR. 2008a. Evidence for Gondwanan vicariance in an ancient clade of gecko lizards. *J Biogeogr* 35:88–104.
- Gamble T, Bauer AM, Greenbaum E, Jackman TR. 2008b. Out of the blue: A novel, trans-Atlantic clade of geckos (Gekkota, Squamata). *Zool Scripta* 37:355–366.
- Gamble T, Bauer AM, Colli GR, Greenbaum E, Jackman TR, Vitt LJ, Simons AM. 2011. Coming to America: Multiple origins of New World geckos. *J Evol Biol* 24:231–244.
- Gamble T, Daza JD, Colli GR, Vitt LJ, Bauer AM. 2011b. A new genus of miniaturized and pug-nosed gecko from South America (Sphaerodactylidae: Gekkota). *Zool J Linnean Soc* 163:1244–1266.
- Gamble T, Greenbaum E, Jackman TR, Russell AP, Bauer AM. 2012. Repeated origin and loss of adhesive toepads in geckos. *PLoS ONE* 7:e39429.
- Gamble T, Coryell J, Ezaz T, Lynch J, Scantlebury D, Zarkower D. 2015a. Restriction site-associated DNA sequencing (RAD-seq) reveals extraordinary number of transitions among gecko sex-determining systems. *Mol Biol Evol* 32:1296–1309.
- Gamble T, Greenbaum E, Jackman TR, Bauer AM. 2015b. Into the light: Diurnality evolved multiple times in geckos. *Biol J Linnean Soc* 115:896–910.
- Garvey W. 1984. Modified elastic tissue-masson trichrome stain. *Stain Techn* 59:213–216.
- Glaw F, Köhler J, Townsend TM, Vences M. 2012. Rivaling the world's smallest reptiles: Discovery of miniaturized and microendemic new species of leaf chameleon (*Brookesia*) from northern Madagascar. *PLoS ONE* 7:e31314.
- Goldschmidt R. 1940. The Material Basis of Evolution. New Haven: Yale University Press.
- Gould SJ. 2002. The Structure of Evolutionary Theory. Cambridge: Belknap Press of Harvard University Press.
- Griffing AH. 2016. Developmental osteology of parafrontal bones in *Aristelliger* and *Teratoscincus* (Squamata: Sphaerodactylidae). Master's Thesis, Villanova University.
- Griffing AH, DeBoer JC, Campbell PD, Wilson BS, Bauer AM. 2017. *Aristelliger praesignis* (Jamaican Croaking Lizard). Maximum Size. *Herpetol Rev* 48:184–185.
- Guerra-Fuentes RA, Daza JD, Bauer AM. 2014. The embryology of the retinal pigmented epithelium in dwarf geckos (Gekkota: Sphaerodactylidae): A unique developmental pattern. *BMC Dev Biol* 14:29.
- Haacke WD. 1975. The burrowing geckos of Southern Africa, 1 (Reptilia: Gekkonidae). *Ann Transvaal Mus* 29:198–243.
- Haines RW, Mohuiddin A. 1968. Metaplastic bone. *J Anat* 103:527–538.
- Han D, Zhou K, Bauer AM. 2004. Phylogenetic relationships among gekkotan lizards inferred from *C-mos* nuclear DNA sequences and a new classification of the Gekkota. *Zool J Linnean Soc* 83: 353–368.
- Hanken J, Wassersug RJ. 1981. The visible skeleton. *Funct Photog* 16:22–26.
- Hecht MK. 1951. Fossil lizards of the West Indian genus *Aristelliger* (Gekkonidae). *Am Mus Novit* 1538:1–33.
- Hedges SB, Thomas R. 2001. At the lower size limit in amniote vertebrates: A new diminutive lizard from the West Indies. *Caribb J Sci* 37:168–173.
- Henderson RW, Powell R. 2009. Natural history of West Indian reptiles and amphibians. Gainesville: University Press of Florida.
- Herrel A, De Vree F, Delheusy V, Gans C. 1999. Cranial kinesis in gekkonid lizards. *J Exp Biol* 202:3687–3698.
- Herrel A, Aerts P, De Vree F. 2000. Cranial kinesis in geckoes: Functional implications. *J Exp Biol* 203:1415–1423.
- Hoogmoed MS. 1973. Notes on the herpetofauna of Surinam. IV. The lizards and amphisbaenians of Surinam. *Biogeographica* 4:1–419.
- Humason GL. 1979. Animal Tissue Techniques. 4th ed. San Francisco: W.H. Freeman and Company.
- Kague E, Roy P, Asselin G, Hu G, Simonet J, Stanley A, Albertson C, Fisher S. 2016. Osterix/Sp7 limits cranial bone initiation sites and is required for formation of sutures. *Dev Biol* 413:160–172.
- Kluge AG. 1967. Higher taxonomic categories of gekkonid lizards and their evolution. *Bull Am Mus Nat Hist* 135:1–60.
- Kluge AG. 1982. Cloacal bones and sacs as evidence of gekkonid lizard relationships. *Herpetologica* 38:348–355.
- Kluge AG. 1983. Cladistic relationships among gekkonid lizards. *Copeia* 1983:465–475.
- Kluge AG. 1987. Cladistic relationships in the Gekkonidae (Squamata, Sauria). *Misc Publ Mus Zool, Univ Mich* 73:1–54.
- Kluge AG. 1995. Cladistic relationships of sphaerodactyl lizards. *Am Mus Novit* 3139:1–23.
- Kok PJR. 2011. A new species of the genus *Gonatodes* Fitzinger, 1843 (Reptilia: Sphaerodactylidae) from central Guyana, northern South America. *Zootaxa* 3018:1–12.
- Largen M, Spawls S. 2010. The Amphibians and Reptiles of Ethiopia and Eritrea. Frankfurt: Chimaira.
- Levrat-Calvia V. 1986–1987. Étude compare des ostéodermes de *Tarentola mauritanica* et de *T. neglecta* (Gekkonidae, Squamata). *Arch Anat Microsc Morphol Exp* 75:29–43.
- Levrat-Calvia V, Zylberberg L. 1986. The structure of the osteoderms in the Gekko: *Tarentola mauritanica*. *Am J Anat* 176:437–446.
- Maderson PFA. 1970. Lizard glands and lizard hands: Models for evolutionary study. *Forma et Functio* 3:179–204.
- McCranie JR, Hedges SB. 2012. Two new species of geckos from Honduras and resurrection of *Sphaerodactylus continentalis* Werner from the synonymy of *Sphaerodactylus millepunctatus* Hallowell (Reptilia, Squamata, Gekkonoidea, Sphaerodactylidae). *Zootaxa* 3492:65–76.
- McCranie JR, Hedges SB. 2013. Two additional new species of *Sphaerodactylus* (Reptilia, Squamata, Gekkonoidea, Sphaerodactylidae) from the Honduran Bay Islands. *Zootaxa* 3694:40–50.
- McDowell SB, Bogert CM. 1954. The systematic position of *Lanthanotus* and the affinities of the anguimorphan lizards. *Bull Am Mus Nat Hist* 105:1–42.
- McNamara KJ. 1986. A guide to the nomenclature of heterochrony. *J Paleo* 60:4–13.
- Meiri S. 2008. Evolution and ecology of lizard body sizes. *Global Ecol Biogeogr* 17:724–734.
- Moczek AP. 2005. The evolution and development of novel traits, or how beetles got their horns. *BioScience* 55:937–951.
- Moczek AP. 2008. On the origins of novelty in development and evolution. *BioEssays* 30:432–447.
- Moczek AP, Cruickshank TE, Shelby A. 2006. When ontogeny reveals what phylogeny hides: Gain and loss of horns during development and evolution of horned beetles. *Evolution* 60:2329–2341.
- Nakashima K, Zhou X, Kunkel G, Zhang Z, Deng JM, Behringer RR, de Crombrugghe B. 2002. The novel zinc finger-containing transcription factor osterix is required for osteoblast differentiation and bone formation. *Cell* 108:17–29.
- Paluh DJ, Griffing AH, Bauer AM. 2017. Sheddable armour: Identification of osteoderms in the integument of *Geckolepis maculata* (Gekkota). *Afr J Herpetol* 66:12–24.
- Peattie AM. 2008. Subdigital setae of narrow-toed geckoes, including a eublepharid (*Aeluroscalabotes felinus*). *Anat Rec* 291:869–875.
- Pyron RA, Burbrink FT, Wiens JJ. 2013. A phylogeny and revised classification of Squamata, including 4161 species of lizards and snakes. *BMC Evol Biol* 13:93.
- R Core Team. 2014. *R: A language and environment for statistical computing*. Vienna, Austria: R Foundation for Statistical Computing. URL: <http://www.R-project.org/>
- Reeder TW, Townsend TM, Mulcahy DG, Noonan BP, Wood PL, Sites JW, Wiens JJ, Wilf P. 2015. Integrated analyses resolve conflicts of squamate reptile phylogeny and reveal unexpected placement fossil taxa. *PLoS ONE* 10:e0118199.
- Rieppel O. 1984a. Miniaturization of the lizard skull: Its functional and evolutionary implications. *Symp Zool Soc Lond* 52:503–520.
- Rieppel O. 1984b. The structure of the skull and jaw adductor musculature in the Gekkota, with comments on phylogenetic

- relationships of the Xantusiidae (Reptilia: Lacertilia). *Zool J Linnean Soc* 82:291–318.
- Rivas GA, Schargel WE. 2008. Gecko on the rocks: An enigmatic new species of *Gonatodes* (Sphaerodactylidae) from Inselbergs of the Venezuelan Guayana. *Zootaxa* 1925:39–50.
- Rivas GA, Ugueto GN, Schargel WE, Barros TR, Velozo P, Sánchez LE. 2013. A distinctive new species of *Gonatodes* (Squamata: Sphaerodactylidae) from Isla La Blanquilla, Venezuela, with remarks on the distribution of some other Caribbean sphaerodactylid lizards. *South Am J Herpetol* 8:5–18.
- Rivero-Blanco C. 1968. Un género y dos especies de Tuqueques (Sauria: Sphaerodactylinae) citados por primera vez para Venezuela, con notas sobre la distribución de otras especies poco conocidas. *Mem Soc Cien Nat LaSalle* (Caracas) 27:103–119.
- Rivero-Blanco C, Schargel WE. 2012. A strikingly polychromatic new species of *Gonatodes* (Squamata: Sphaerodactylidae) from northern Venezuela. *Zootaxa* 3518:66–78.
- Rojas-Runjaic FJM, Infante-Rivero EE, Cabello P, Velozo P. 2010. A new non-sexually dichromatic species of the genus *Gonatodes* (Sauria: Sphaerodactylidae) from Sierra de Perijá, Venezuela. *Zootaxa* 2671:1–16.
- Röll B. 2001. Gecko vision—retinal organization, foveae and implications for binocular vision. *Vision Res* 41:2043–2056.
- Rösler H, Köhler J, Böhme W. 2008. A new species of diurnal gekkonid genus *Pristurus* Rüppell, 1835 from the Red Sea island Hanish al-Kabir, Yemen. *Amphibia-Reptilia* 29:217–227.
- Russell AP. 1979. Parallelism and integrated design in the foot structure of gekkonine and diplodactyline geckos. *Copeia* 1979:1–21.
- Schargel WE, Rivas GA, Makowsky R, Señaris JC, Natera MA, Barros TR, Molina CR, Barrio-Amorós CL. 2010. Phylogenetic Systematics of the genus *Gonatodes* (Squamata: Sphaerodactylidae) in the Guayana region, with description of a new species from Venezuela. *Syst Biodivers* 8:321–339.
- Scherz MD, Daza JD, Köhler J, Vences M, Glaw F. 2017. Off the scale: A new species of fish-scale gecko (Squamata: Gekkonidae: *Geckolepis*) with exceptionally large scales. *PeerJ* 5:e2955.
- Schindelin J, Arganda-Carreras I, Frise E, Kaynig V, Longair M, Pietzsch T, Preibisch S, Rueden C, Saalfeld S, Schmid B, et al. 2012. Fiji: An open-source platform for biological-image analysis. *Nat Meth* 9:676–682.
- Schleich HH, Kästle W, Kabisch K. 1996. Amphibians and Reptiles of North Africa. Koenigstein: Koeltz.
- SchwartzA, Henderson RW. 1991. Amphibians and Reptiles of the West Indies: Descriptions, Distributions, and Natural History. Gainesville: University Press of Florida.
- Sire J-Y, Donoghue PCJ, Vickaryous MK. 2009. Origin and evolution of the integumentary skeleton in non-tetrapod vertebrates. *J Anat* 214:409–440.
- Stephenson NG, Stephenson EM. 1956. The osteology of New Zealand geckos and its bearing on their morphological status. *Trans Proc R Soc N Z* 84:341–358.
- Stewart GR, Daniel RS. 1972. Scales of the lizard *Gekko gecko*: Surface structure examined with the scanning electron microscope. *Copeia* 1972:252–257.
- Sturaro MJ, Avila-Pires TCS. 2011. Taxonomic revision of the geckos of the *Gonatodes concinnatus* complex (Squamata: Sphaerodactylidae), with description of two new species. *Zootaxa* 2869:1–36.
- Szczerbak MM, Golubev ML. 1996. Gecko Fauna of the USSR and Contiguous Regions. St. Louis: Society for the Study of Amphibians and Reptiles.
- Thomas R. 1975. The *argus* group of West Indian *Sphaerodactylus* (Sauria: Gekkonidae). *Herpetologica* 31:177–195.
- Uetz P, Freed P, Hošek J. 2017. The Reptile Database, <http://www.reptile-database.org>, accessed January 18, 2017.
- Underwood G. 2010. On the classification and evolution of geckos. *Proc Zool Soc Lond* 124:469–492.
- Vickaryous MK, Hall BK. 2008. Development of the dermal skeleton in *Alligator mississippiensis* (Archosauria, Crocodylia) with comments on the homology of osteoderms. *J Morphol* 269:398–422.
- Vickaryous MK, Meldrum G, Russell AP. 2015. Armored geckos: A histological investigation of osteoderm development in *Tarentola* (Phyllodactylidae) and *Gekko* (Gekkonidae) with comments on their regeneration and inferred function. *J Morphol* 276:1345–1357.
- Wagner GP. 1989. The origin of morphological characters and the biological basis of homology. *Evolution* 43:1157–1171.
- Wake DB, Wake MH, Specht CD. 2011. Homoplasy: From detecting pattern to determining process and mechanism of evolution. *Science* 331:1032–1035.
- Wassersug RJ. 1976. A procedure for differential staining of cartilage and bone in whole formalin-fixed vertebrates. *Biotech Histochem* 51:131–134.
- Werner F. 1896. Beiträge zur Kenntnis der Reptilien und Batrachier von Centralamerika und Chile, sowie einiger seltenerer Schlangenarten. *Verh Zool-Bot Ges Wien* 46:344–365.
- Wise PA, Russell AP. 2010. Development of the dorsal circumorbital bones in the leopard gecko (*Eublepharis macularius*) and its bearing on the homology of these elements in the gekkota. *Anat Rec* 293:2001–2006.